



Rational design of carbamate-based dual binding site and central AChE inhibitors by a “biooxidisable” prodrug approach: Synthesis, in vitro evaluation and docking studies

Mihaela-Liliana Țîntaş, Vincent Gembus, Florent Alix, Anaïs Barré, Gaël Coadou, Lina Truong, Muriel Sebban, Cyril Papamicaël, Hassan Oulyadi, Vincent Levacher

► To cite this version:

Mihaela-Liliana Țîntaş, Vincent Gembus, Florent Alix, Anaïs Barré, Gaël Coadou, et al.. Rational design of carbamate-based dual binding site and central AChE inhibitors by a “biooxidisable” prodrug approach: Synthesis, in vitro evaluation and docking studies. *European Journal of Medicinal Chemistry*, 2018, 155, pp.171-182. 10.1016/j.ejmech.2018.05.057 . hal-03134356

HAL Id: hal-03134356

<https://hal.science/hal-03134356>

Submitted on 8 Feb 2021

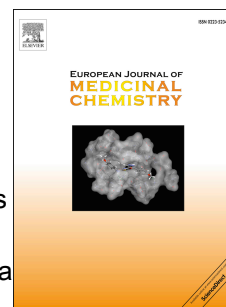
HAL is a multi-disciplinary open access archive for the deposit and dissemination of scientific research documents, whether they are published or not. The documents may come from teaching and research institutions in France or abroad, or from public or private research centers.

L'archive ouverte pluridisciplinaire **HAL**, est destinée au dépôt et à la diffusion de documents scientifiques de niveau recherche, publiés ou non, émanant des établissements d'enseignement et de recherche français ou étrangers, des laboratoires publics ou privés.

Accepted Manuscript

Rational design of carbamate-based dual binding site and central AChE inhibitors by a “biooxidisable” prodrug approach: Synthesis, *in vitro* evaluation and docking studies

Mihaela-Liliana Țîntăș, Vincent Gembus, Florent Alix, Anaïs Barré, Gaël Coadou, Lina Truong, Muriel Sebban, Cyril Papamicaël, Hassan Oulyadi, Vincent Levacher



PII: S0223-5234(18)30488-4

DOI: [10.1016/j.ejmech.2018.05.057](https://doi.org/10.1016/j.ejmech.2018.05.057)

Reference: EJMECH 10468

To appear in: *European Journal of Medicinal Chemistry*

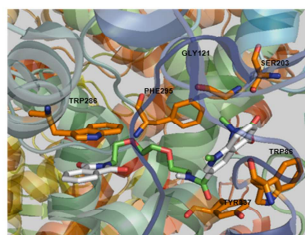
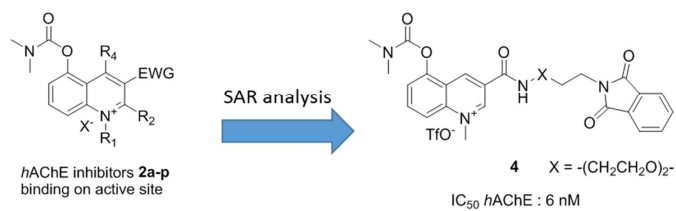
Received Date: 16 February 2018

Revised Date: 10 April 2018

Accepted Date: 31 May 2018

Please cite this article as: M.-L. Țîntăș, V. Gembus, F. Alix, Anaïs Barré, Gaël Coadou, L. Truong, M. Sebban, C. Papamicaël, H. Oulyadi, V. Levacher, Rational design of carbamate-based dual binding site and central AChE inhibitors by a “biooxidisable” prodrug approach: Synthesis, *in vitro* evaluation and docking studies, *European Journal of Medicinal Chemistry* (2018), doi: 10.1016/j.ejmech.2018.05.057.

This is a PDF file of an unedited manuscript that has been accepted for publication. As a service to our customers we are providing this early version of the manuscript. The manuscript will undergo copyediting, typesetting, and review of the resulting proof before it is published in its final form. Please note that during the production process errors may be discovered which could affect the content, and all legal disclaimers that apply to the journal pertain.



- Synthesis and SAR evaluation of compounds **2a-p**
- *In vitro* evaluation of **4** and its prodrug **3** against hAChE activity
- Molecular docking simulation of **4**

Rational design of carbamate-based dual binding site and central AChE inhibitors by a “biooxidisable” prodrug approach: synthesis, in vitro evaluation and docking studies

Mihaela-Liliana Țîntaş^b, Vincent Gembus^{*a}, Florent Alix ^a, Anaïs Barré^{a,b}, Gaël Coadou^b,
Lina Truong^b, Muriel Sebban^b, Cyril Papamicaël^b, Hassan Oulyadi^b, Vincent Levacher^{*b}

^aVFP Therapies, 15 rue François Couperin, 76000 Rouen, France

^bNormandie Univ, UNIROUEN, INSA Rouen, CNRS, COBRA, 76000 Rouen, France

*Corresponding authors : Vincent Levacher, tel/fax : +33235522485/+33235522462, e-mail: vincent.levacher@insa-rouen.fr ; Vincent Gembus, tel/fax : +33235522465/+33235522462, e-mail: vgembus@vfp-therapies.com

ABSTRACT

Herein, we report a new class of dual binding site AChE inhibitor **4** designed to exert a central cholinergic activation thanks to a redox-activation step of a prodrug precursor **3**. Starting from potent pseudo-irreversible quinolinium salts AChE inhibitors **2** previously reported, a new set of diversely substituted quinolinium salts **2a-p** was prepared and assayed for their inhibitory activity against AChE. Structure-activity relationship (SAR) analysis of **2a-p** coupled with molecular docking studies allowed us to determine which position of the quinolinium scaffold may be considered to anchor the phthalimide fragment presumed to interact with the peripheral anionic site (PAS). In addition, molecular docking provided insight on the linker length required to connect both quinolinium and phthalimide moieties without disrupting the crucial role of quinolinium salt moiety within the catalytic active site (CAS); namely placing the carbamate in the correct position to trigger carbamylation of the active-site serine hydroxyl. Based on this rational design, the putative dual binding site inhibitor **4** and its prodrug **3** were synthesized and subsequently evaluated *in vitro* against AChE. Pleasingly, whereas

compound **4** showed to be a highly potent inhibitor of AChE ($IC_{50} = 6$ nM) and binds to AChE-PAS to the same extent as donepezil, its prodrug **3** revealed to be inactive ($IC_{50} > 10$ μ M). These preliminary results constitute one of the few examples of carbamate-based dual binding site AChE inhibitors.

Keywords: Acetylcholine esterase inhibitors, Alzheimer, Dual-binding site inhibitor

1. Introduction

Alzheimer's disease (AD) is the most common cause of dementia characterized among other things by the central cholinergic depletion and amyloid- β ($A\beta$) plaques [1-2]. So far, the use of acetylcholinesterase (AChE) inhibitors has dominated the symptomatic treatment in early-to-moderate AD [3]. There are currently three marketed drugs, namely donepezil, rivastigmine and galantamine. These three molecules, associated in some cases with memantine (NMDA antagonist glutamate) are the only therapeutic arsenal commercially available. Much efforts have been devoted these last years to develop dual binding site AChE inhibitors that simultaneously bind to both catalytic active site (CAS) and peripheral anionic site (PAS) of the enzyme [4-20]. Indeed, it was postulated that PAS of the enzyme binds to the nonamyloidogenic form of $A\beta$ protein inducing conformational changes and subsequent amyloid fibril formation [21-23]. As a result, these new AChE inhibitors are expected to exhibit a better pharmacological profile in that they may not only alleviate cognitive deficits but also slow down the progression of AD by inhibiting the $A\beta$ peptide aggregation. Although these findings triggered a renewed interest in the development for AChE inhibitors, the fact remains that peripheral activity commonly encountered with AChE inhibitors causes severe adverse effects and limit seriously their therapeutic efficiency [24]. To address this issue, we recently reported "biooxidisable" prodrugs **1** derived from rivastigmine with the aim at improving brain delivery and therapeutic efficacy of AChE inhibitors [25-26]. This prodrug

approach is based on the masking of a positive charge which is involved in a cation- π interaction with Trp84 within the catalytic site of AChE. In contrast to rivastigmine, it is hypothesized that the dihydroquinoline prodrug **1** remains unprotonated at physiological pH, thus masking the crucial positive charge while ensuring a good lipophilicity to cross the blood-brain barrier (BBB). Once in the brain, oxidation of the dihydroquinoline **1** would unmask the permanent positive charge to restore central AChE inhibition while avoiding the resulting quinolinium salt **2** to cross back the BBB by passive diffusion (Figure 1a). Although most carbamate quinolinium salts **2** were potent against *h*AChE (IC_{50} up to 10 nM), all corresponding 1,4-dihydroquinolines proved to be unable to inhibit *h*AChE ($IC_{50} > 10 \mu M$), providing an *in vitro* proof of concept of this prodrug approach. In this context, we report herein the rational design of new central dual binding site AChE inhibitors **4** by exploiting this “biooxidisable” prodrug approach as depicted in Figure 1b. These dual binding site AChE inhibitors are expected to restore the cholinergic transmission and prevent the aggregation of A β , all the while avoiding deleterious peripheral effects frequently encountered in the treatment of AD.

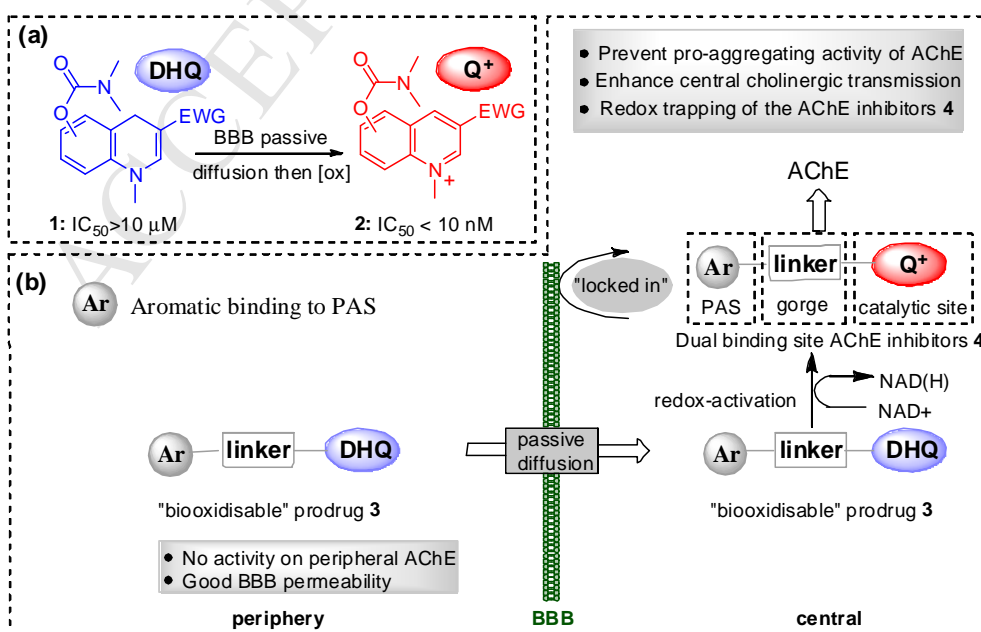


Figure 1. Design of central AChE inhibitors by a “biooxidisable” prodrug approach (a) catalytic site AChE inhibitors (prior work); (b) dual binding site AChE inhibitors (this work).

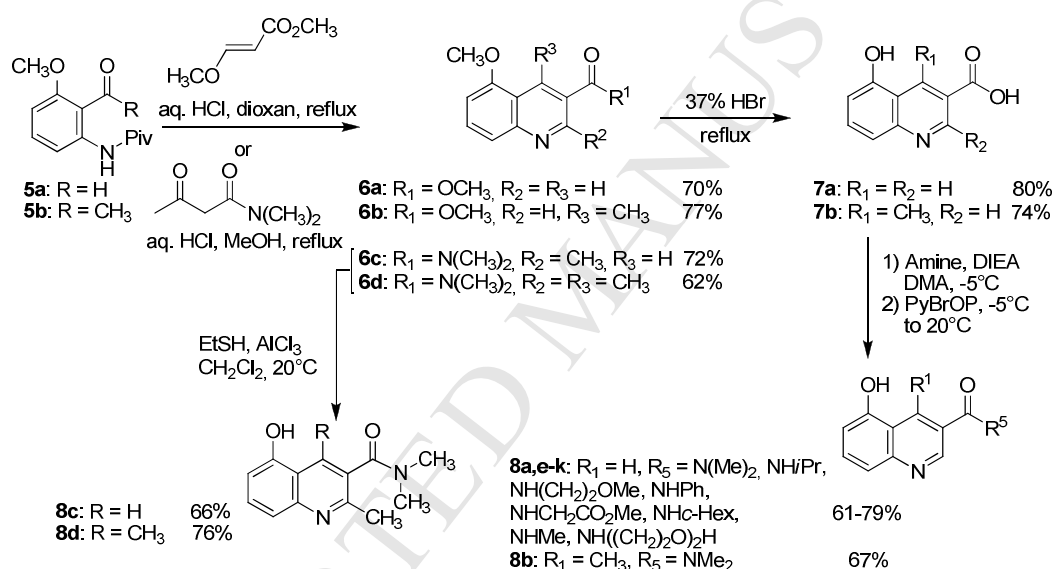
2. Results and discussion

2.1. Synthesis of quinolinium salts 2a-p

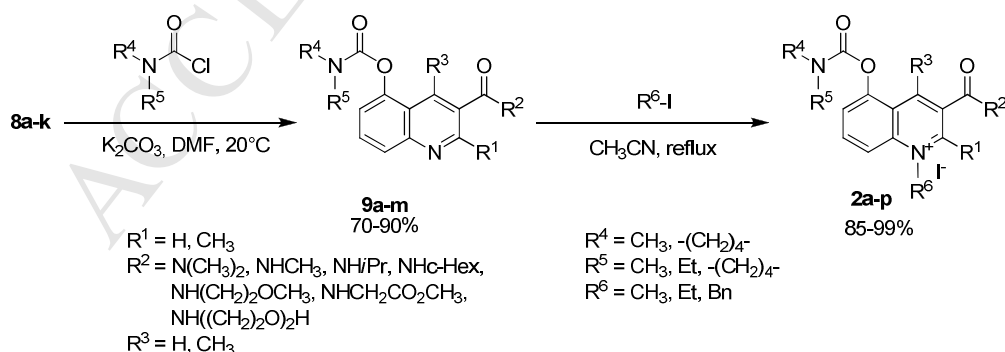
These central dual binding site AChE inhibitors **4** are made up of a carbamate quinolinium salt moiety connected via a linker to an aromatic fragment to bind to the PAS of AChE. We had first to figure out how and where to connect the aromatic fragment with the quinolinium salt moiety. From our previous work [25], some structure-activity relationship (SAR) information was already available to us to address this challenge; namely that the best AChE inhibitory activities were obtained when the carbamate group of quinolinium salts **2** is located at C-5. To probe which region of the inhibitor may be considered to link a spacer without causing major disruptions on the AChE inhibitory activity, we embarked on the preparation of a new series of carbamate quinolinium salts **2a-p**.

The general synthetic route to target compounds **2a-p** involves a classical Friedländer approach followed by an appropriate multi-step functionalization sequence of the resulting 5-methoxyquinoline derivatives (Schemes 1-2). Thus, quinoline esters **6a,b** were readily prepared in 70-77% yields by reacting methyl *trans*-3-methoxyacrylate with 2-aminobenzaldehyde **5a** and 2-aminoacetophenone **5b** respectively. Likewise, quinoline carboxamides **6c,d** were prepared from *N,N*-dimethylacetoacetamide and compounds **5a,b** in 62-72% yields. The resulting 5-methoxyquinoline esters **6a,b** were subjected to *O*-demethylation in refluxing concentrated HBr to furnish the corresponding 5-hydroxyquinoline-3-carboxylic acids **7a,b** in 74-80% yields. Furthermore, smooth *O*-demethylation of 5-methoxyquinoline-3-*N,N*-dimethylcarboxamides **6c,d** took place by means of ethanethiol and aluminium chloride [27] and without reacting with the carboxamide

function at C-3, thus providing 5-hydroxyquinoline-3-*N,N*-dimethylcarboxamides **8c,d** in 66-76% yields. Additionally, a panel of 5-hydroxyquinoline-3-carboxamides **8a,b,e-k** could be prepared in 61-79% yields from 5-hydroxyquinoline-3-carboxylic acids **7a,b** and various amines in the presence of PyBroP as coupling agent (Scheme 1). Lastly, carbamylation of the resulting 5-hydroxyquinoline-3-carboxamides **8a-k** afforded the corresponding 5-carbamylated quinoline-3-carboxamides **9a-m** in 70-90% yields which were subsequently quaternized to give rise to the desired target quinolinium salts **2a-p** in high yields (85-99%) (Scheme 2).



Scheme 1. Synthesis of 5-hydroxyquinoline-carboxamides **8a-k**.



Scheme 2. Access to quinolinium salts **2a-p** - carbamylation and quaternization steps.

2.2. *In vitro* evaluation of compounds 2a-p, SAR analysis and docking

In vitro hAChE inhibitory activity of these new quinolinium salts **2a-p** was evaluated using the classical Ellman's assay [28]. Preliminary SAR analysis indicated that substitution at C-2 or/and C-4 by a methyl group resulted in a complete loss of AChE inhibitory activity (Fig. **2a**). Second, the inhibiting activity drops sharply when the *N*-substituent of the quinolinium salt increases in size (Fig. **2b**). We also looked at the nature of the carbamate and showed that only *N,N*-dimethyl carbamate exhibits an AChE inhibitory activity, all structural modifications at the carbamate moiety leading to a collapse of the AChE inhibitory activity (Fig. **2c**). This finding is likely related to the inhibition mechanism of these pseudo-irreversible AChE inhibitors, transferring the carbamate moiety to the serine hydroxyl group at the esterase site of the enzyme. Interestingly, we investigated the nature of the electron withdrawing group at C-3 and showed that quite large structural variations at this position are tolerated without compromising as much hAChE inhibition; IC₅₀ values ranging from 20 to 93 nM (Fig. **2d**). It is worth mentioning that this functional group was deemed essential to ensure some stability of the corresponding prodrugs **1** at the periphery by protecting the enamine double bond against electrophilic attack.

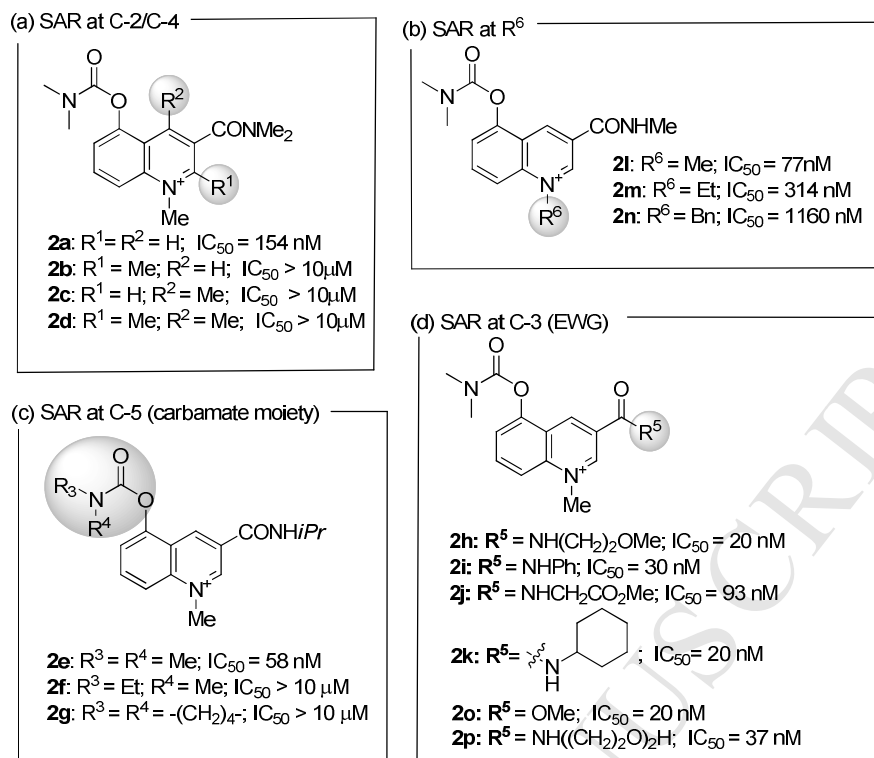


Figure 2. Structure-activity relationship of carbamate-quinolinium salts **2a-p** – In vitro *hAChE* inhibition assay (Ellman's test).

Analysis of this SAR data prompted us to suggest that the functional group located at C-3 is likely the most appropriate attachment-point to link the aromatic fragment to the quinolinium salt. Moreover, this assumption was supported by a molecular docking simulation study of compounds **2h**, **2j**, **2k** and **2p** on *TcAChE* (PDB ID: 2CKM) (Figure 3A-D). For all compounds, the docking interactions showed that the carbamate group is pointing towards Ser200 residue present in the active site of *TcAChE*. It was also observed a strong nitrogen cation- π interaction and π - π stacking with Phe330 amino acid and π - π stacking between quinolinium and indole ring of Trp84. These interactions position the structure of the quinolinium compounds in the active site such that the substituent in C-3 position is located near the bottom of the hydrophobic gorge and can thus allow the chain to be elongated towards PAS.

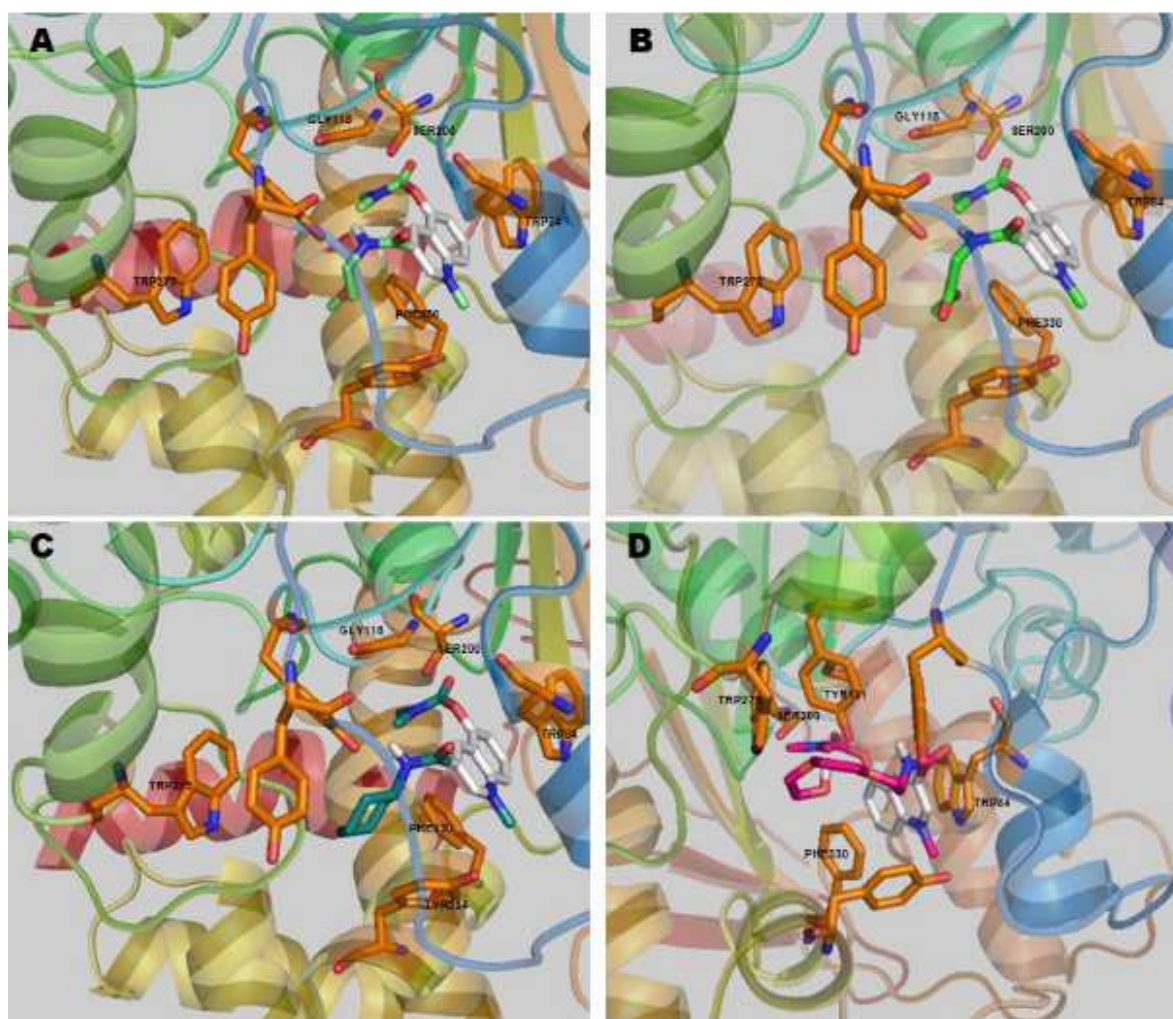


Figure 3. Top-scored poses obtained with Autodock Vina [29] for compounds **2h** (A), **2j** (B), **2k** (C) and **2p** (D) positioned in active site of *TcAChE* (PDB ID: 2CKM). The compounds and the selected side chains of the binding site residues are in stick and the protein in cartoon representation. This figure was made with PyMol [30].

2.3. Docking, synthesis and *in vitro* evaluation of compound **4** and its prodrug **3**

Armed with this valuable SAR study, quinolinium-phthalimide heterodimer **4** was proposed as a putative dual binding site AChE inhibitor (Figure 4). The proposed heterodimeric AChE inhibitors **4** contain a phthalimide moiety which is clearly highlighted in the literature as being one of the most popular aromatic fragments for binding to the PAS region of AChE. [31-34]

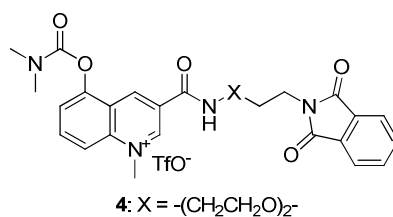


Figure 4. Quinolinium-phthalimide heterodimer **4**.

We next examined from a docking simulation study with *TcAChE* (PDB ID: 2CKM) whether the polyethylene glycol (PEG)-based spacer length in heterodimer **4** makes it possible for quinolinium and phthalimide fragments to simultaneously bind to the CAS and the PAS respectively. A detailed analysis of the binding mode of the best docked conformation highlights dual-binding mode of action; while the quinolinium moiety interacts with the CAS through aromatic interactions with Trp84 and Phe330 leading the carbamate group to point towards Ser200, the PEG linker goes up the aromatic gorge and the phthalimide core binds by π -stacking to both Tyr70 and Trp279 PAS residues (Figure 5A). In addition, a docking simulation of compound **4** with *rhAChE* (PDB ID: 4EY7) was also achieved and the best-scored pose confirmed the preceding results; namely strong interactions with both CAS and PAS amino-acid residues (Figure 5B).

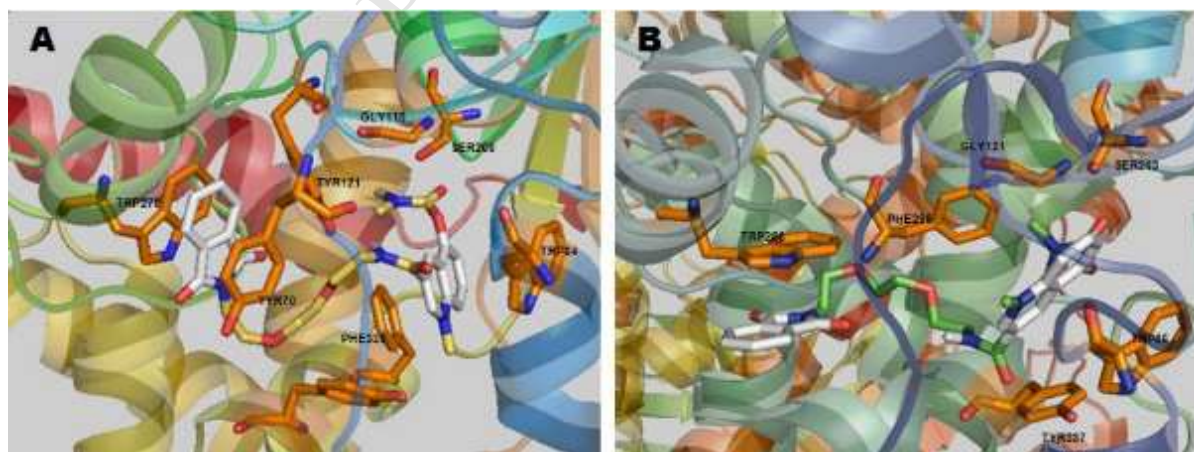
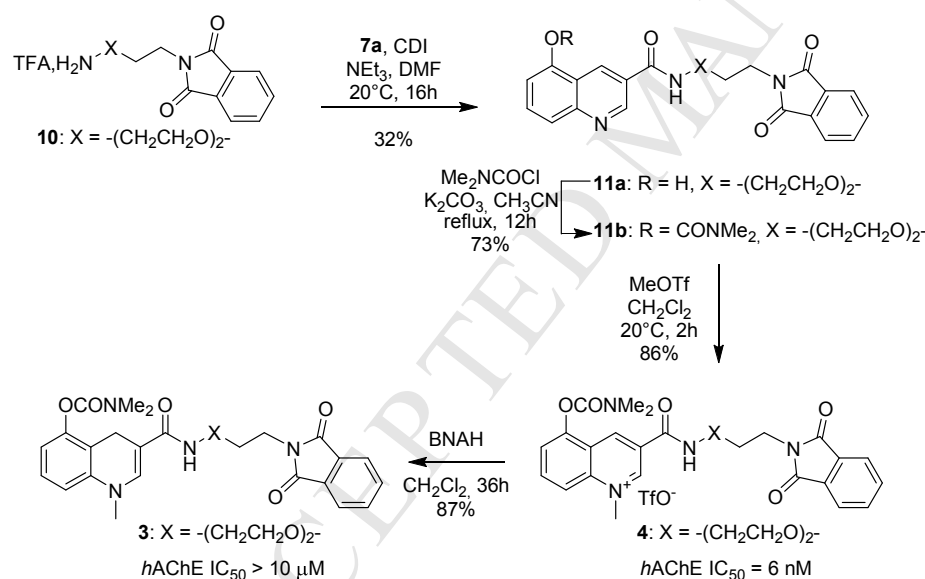


Figure 5. Top-scored poses obtained with Autodock Vina [29] for compound **4** positioned in active site of *TcAChE* (Figure 5A, PDB ID: 2CKM) and in *rhAChE* (Figure 5B, PDB ID: 4EY7). The compounds and the selected side chains of the binding site residues are in stick and the protein in cartoon representation. This figure was made with PyMol [30].

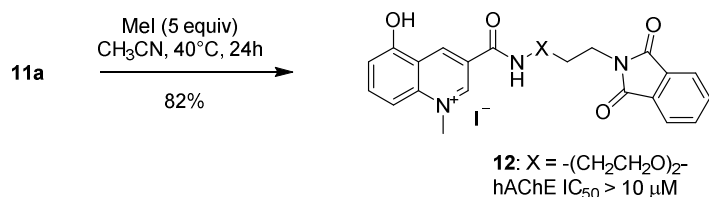
Supported by these promising predictions, we embarked on the synthesis of quinolinium-phthalimide heterodimer **4** (Scheme 3). The phthalimide-amine **10** [35] and 5-hydroxyquinoline-3-carboxylic acid **7a** were treated with CDI to afford the expected quinoline-phthalimide **11a** in 32% yield. All attempts to increase the yield by using other coupling agents such as HATU or HBTU failed, leading to poorly reproducible yields and tedious purifications. Subsequent carbamylation of **11a** afforded 5-carbamylated quinoline-phthalimide **11b** in good yield (73%) which was readily converted to the corresponding quinolinium salt **4** in 86% yield in the presence of MeOTf as quaternization reagent. Finally, the putative prodrug **3** was obtained by regioselective 1,4-reduction of **4** with 1-benzyl-1,4-dihydronicotinamide (BNAH).



Scheme 3. Synthesis and *hAChE* inhibitory activity of dual binding site AChE inhibitor **4** and its prodrug **3**.

Pleasingly, whereas ligand **4** showed to be a potent *hAChE* inhibitor (IC₅₀ = 6 nM, Ellman's test [28]), its "biooxidisable" prodrug form **3** revealed no inhibitory activity towards the enzyme (IC₅₀ > 10 μM). Pleasingly, the prodrug also displayed good permeability in Caco-2 assay (P_{app} (A-B) = 11.1x10⁻⁶ cm/s, recovery = 91 %). More importantly, ligand **4** showed to

displace propidium iodide from the PAS of *hAChE* (20%) and to inhibit the A β (1-42) self-aggregation (14% at 10 μ M) to the same extent as donepezil [36]. In addition, compound **12** was also prepared by reaction with methyl iodide in acetonitrile at 40°C (Scheme 4). It was proved to be inactive against *hAChE* activity, i.e. 35% inhibition at 10⁻⁵M, confirming the crucial role of carbamate group in the enhancement of the anti-AChE activity.



Scheme 4. Synthesis and *hAChE* inhibitory activity of quinolinium **12**.

These preliminary *in vitro* assays allow not only to identify a novel class of highly potent heterodimeric *hAChE* inhibitors, but also to consider further development of highly centrally active dual binding site *hAChE* inhibitors with increased efficacy and/or decreased side effects by means of a “biooxidisable” prodrug approach.

3. Conclusion

From our previous work dealing with central pseudo-irreversible AChE inhibitors based on a redox-activated prodrug strategy [25-26], a new quinolinium-phthalimide heterodimeric ligand **4** was designed to simultaneously interact with both the active and peripheral sites of AChE. By means of a SAR study of diverse synthesized quinolinium salts **2a-p** and a molecular docking simulation of compounds **2h**, **2j**, **2k** and **2p**, we could determine which position of the quiniolium ring is the most suitable to attach the PEG linker so that the phthalimide fragment at its end is able to interact with the PAS of *hAChE*. After docking simulation of the designed heterodimer **4** in *hAChE* showing a possible dual-site binding fashion, ligand **4** was efficiently prepared and revealed to be highly potent against *hAChE* activity (IC₅₀ = 6 nM)

while the corresponding prodrug **3** turned out to be inactive ($IC_{50} > 10 \mu M$). Moreover, a propidium competition assay confirms the interaction of compound **4** at the PAS inducing A β (1-42) self-aggregation inhibitory activities. All together, these findings pave the way for the development of novel and side-effects free prodrugs of potent dual binding site AChE inhibitors for the treatment of amnesic disorders like Alzheimer disease.

4. Experimental section

4.1. General

All commercial reagents were used without further purification. The solvents were dried with appropriate desiccants and distilled prior to use or were obtained anhydrous from commercial suppliers. Silica gel (60, 230–400 mesh or 70–230 mesh) was used for column chromatography. Reactions were monitored by thin layer chromatography on silica gel precoated aluminum plates. UV light at 254 nm or $KMnO_4$ stains were used to visualize TLC plates. 1H , ^{13}C NMR spectra were recorded using a spectrometer operating at 300 and 75 MHz respectively. Abbreviations used for peak multiplicities are s: singlet, d: doublet, t: triplet, q: quadruplet dd = doublet of doublet, br = broad, dq = doublet of quadruplet and m: multiplet. Coupling constants J are in Hz and chemical shifts are given in ppm and calibrated with $DMSO-d_6$ or $CDCl_3$ (residual solvent signals). 1H NMR spectra obtained in $CDCl_3$ were referenced to 7.26 ppm. ^{13}C NMR spectra obtained in $CDCl_3$ were referenced to 77.16 ppm and in $DMSO-d_6$ were referenced to 39.52 ppm. High-resolution mass spectrometry (HRMS) was carried out on a waters LCT XE spectrometer. Elemental analyses were performed by the microanalysis service of the University of Rouen and were recorded with a Thermo Scientific FLASH 2000 analyzer.

Derivatives **5a,b** were synthesized from 3-anisidine using a previously described synthesis.[37-38] Compounds **6a**, **7a**, **2o** were prepared according to the same procedure as we have already reported in the literature. [25]

4.2. Chemistry

4.2.1. Methyl 5-methoxy-4-methyl-quinoline-3-carboxylate (**6b**)

To a solution of ketone **5b** (7.73 g, 31.0 mmol) and methyl *trans*-3-methoxyacrylate (7.4 mL, 68.4 mmol) dissolved in 150 mL of methanol was slowly added 3M aqueous solution of hydrochloric acid (100 mL). The resulting mixture was stirred under reflux for 3 hours, then cooled to room temperature and neutralized by adding solid Na₂CO₃. The aqueous solution was extracted with CH₂Cl₂ (4x150 mL) and the combined organic layers were dried (MgSO₄), filtered and concentrated under vacuum. The crude product was then filtered on silica gel to afford 5.52 g of quinoline **6b**. Pale yellow solid, yield: 77%. Mp 85°C. *R*_f = 0.39 (Petroleum ether:EtOAc 1:1). ¹H NMR (300 MHz, CDCl₃) δ 9.03 (s, 1H), 7.67-7.58 (m, 2H), 6.87 (dd, *J* = 7.5 Hz, *J* = 1.5 Hz, 1H), 3.96 (s, 3H), 3.93 (s, 3H), 3.04 (s, 3H). ¹³C NMR (CDCl₃) δ 168.0, 158.6, 150.5, 149.8, 148.7, 130.8, 124.9, 122.4, 120.4, 106.4, 55.7, 52.5, 20.6. HRMS (ESI+) mass calcd for [M+H]⁺ C₁₃H₁₄NO₃ *m/z* 232.0973, found 232.0964.

4.2.2. General procedure for reaction with *N,N*-dimethylacetoacetamide (**6c-d**)

To a solution of aldehyde **5a** or ketone **5b** (4.0 mmol) and *N,N*-dimethylacetoacetamide (0.49 mL, 4.0 mmol) dissolved in 20 mL of dioxan was slowly added 37% aqueous hydrochloric acid (6 mL). The resulting mixture was stirred under reflux for 6 hours, then cooled to room temperature and neutralized by adding solid K₂CO₃. The aqueous solution was extracted with

CH₂Cl₂ (4x15 mL) and the combined organic layers were dried (MgSO₄), filtered and concentrated under vacuum. The crude product was purified by chromatography on silica gel to afford quinolines **6c** or **6d**.

4.2.2.1. 5-Methoxy-*N,N*,2-trimethyl-quinoline-3-carboxamide (**6c**)

Pale brown solid, yield: 72%. Mp 126°C. *R_f* = 0.15 (EtOAc). ¹H NMR (300 MHz, CDCl₃) δ 8.38 (s, 1H), 7.62-7.56 (m, 2H), 6.81 (dd, *J* = 4.8 Hz, *J* = 2.7 Hz, 1H), 3.96 (s, 3H), 3.17 (s, 3H), 2.87 (s, 3H), 2.67 (s, 3H) ppm. ¹³C NMR (75 MHz, CDCl₃) δ 170.0, 155.3, 148.4, 130.3, 129.4, 128.7, 120.7, 118.3, 104.3, 55.8, 38.7, 34.9, 23.1 ppm. HRMS (ESI+) mass calcd for [M+H]⁺ C₁₄H₁₇N₂O₂ *m/z* 245.1290, found 245.1279.

4.2.2.2. 5-Methoxy-*N,N*,2,4-tetramethyl-quinoline-3-carboxamide (**6d**)

Pale brown solid, yield: 62%. Mp 112°C. *R_f* = 0.12 (EtOAc). ¹H NMR (300 MHz, CDCl₃) δ 7.61-7.52 (m, 2H), 6.83 (dd, *J* = 7.5 Hz, *J* = 1.5 Hz, 1H), 3.93 (s, 3H), 3.21 (s, 3H), 2.82 (s, 3H), 2.76 (s, 3H), 2.58 (s, 3H) ppm. ¹³C NMR (75 MHz, CDCl₃) δ 170.3, 157.9, 154.2, 149.1, 141.5, 130.5, 129.5, 121.6, 118.6, 105.5, 55.5, 37.6, 34.5, 22.9, 20.3 ppm. HRMS (ESI+) mass calcd for [M+H]⁺ C₁₅H₁₉N₂O₂ *m/z* 259.1446, found 259.1443.

4.2.3. 5-Hydroxy-4-methyl-quinoline-3-carboxylic acid (**7b**)

A solution of ester **6b** (5.45 g, 23.6 mmol) in an aqueous solution of HBr (150 mL, 48%) was heated under reflux for 24 hours. After cooling the reaction mixture to room temperature, the pH was adjusted to 2 with 2M aqueous NaOH. After filtration of the insoluble matter, the pH was adjusted between 5 and 6, and the resulting precipitate was filtered off, rinsed with cooled

water and dried at 50°C under vacuum to afford 3.55 g of carboxylic acid **7b**. Brown solid, yield: 74%. Mp 210°C. ¹H NMR (300 MHz, DMSO-*d*₆) δ 8.89 (s, 1H), 7.55 (t, *J* = 8.1 Hz, 1H), 7.44 (d, *J* = 8.1 Hz, 1H), 7.01 (d, *J* = 7.5 Hz, 1H), 3.06 (s, 3H) ppm. ¹³C NMR (75 MHz, DMSO-*d*₆) δ 168.8, 156.9, 150.1, 149.3, 147.1, 131.1, 125.4, 120.1, 118.7, 111.2, 20.0 ppm. Found: C, 64.9; H, 4.45; N, 6.80. Calc. for C₁₁H₉NO₃: C, 65.02; H, 4.46; N, 6.89%.

4.2.4. General procedure for demethylation of 5-methoxy-quinolines derivatives with AlCl₃

Under Argon Atmosphere, AlCl₃ (1.41 g, 5 equiv) were placed in suspension in 2.5 mL of DCM. The suspension was cooled at 0°C then ethanethiol (1.7 mL, 10.8 equiv) was dropwise added following by the addition of substrate (1.0 mmol, 1 equiv) in DCM (9 mL). After stirring overnight at room temperature, a Rochelle's salt solution was added at room temperature and the mixture was extracted five times with DCM. The combined organic phase was dried over MgSO₄ and concentrated under vacuum to give the expected compound.

4.2.4.1. 5-Hydroxy-*N,N*,2-trimethyl-quinoline-3-carboxamide (**8c**)

Brown solid, yield: 66%. Mp 95°C. *R_f* = 0.09 (EtOAc). ¹H NMR (300 MHz, CDCl₃) δ 8.47 (s, 1H), 7.45 (d, *J* = 8.1 Hz, 1H), 7.35 (t, *J* = 7.5 Hz, 1H), 6.82 (d, *J* = 6.6 Hz, 1H), 3.18 (s, 3H), 2.89 (s, 3H), 2.69 (s, 3H) ppm. ¹³C NMR (75 MHz, CDCl₃) δ 169.9, 154.5, 153.7, 146.6, 132.0, 131.3, 128.2, 118.2, 117.2, 109.9, 39.0, 35.1, 21.9 ppm. HRMS (ESI+) mass calcd for [M+H]⁺ C₁₃H₁₅N₂O₂ *m/z* 231.1133, found 231.1124.

4.2.4.2. 5-Hydroxy-*N,N*,2,4-tetramethyl-quinoline-3-carboxamide (**8d**)

Pale brown solid, yield: 76%. Mp 99°C. R_f = 0.1 (EtOAc). ^1H NMR (300 MHz, MeOD) δ 11.05 (br s, 1H), 8.72-8.64 (m, 2H), 8.15 (dd, J = 6.0 Hz, J = 3.0 Hz, 1H), 4.42 (s, 3H), 4.14 (s, 3H), 4.02 (s, 3H), 3.74 (s, 3H) ppm. ^{13}C NMR (75 MHz, MeOD) δ 172.1, 157.7, 155.0, 150.0, 144.5, 131.6, 130.9, 119.8, 118.9, 111.4, 38.2, 34.8, 22.5, 20.5 ppm. HRMS (ESI+) mass calcd for $[\text{M}+\text{H}]^+$ $\text{C}_{14}\text{H}_{17}\text{N}_2\text{O}_2$ m/z 245.1290, found 245.1286.

4.2.5. General procedure for amidation of carboxylic acid

A suspension of carboxylic acid **7a** or **7b** (1.0 mmol) in anhydrous DMA (5 mL) was heated to 50°C until complete solubilisation then the resulting solution was cooled to -5 °C. Amine (1.0 mmol, 1 equiv) and DIEA (0.52 mL, 3.0 mmol) were then added followed by PyBrop (466.2 mg, 1.0 mmol) in one portion. The mixture was then warmed to room temperature and stirred for up to 15 h. Water (3 mL) was added dropwise at 0°C and the mixture was neutralized with a saturated aqueous solution of ammonium chloride. The product was extracted with EtOAc (5x) and the combined organic layers washed with brine (2x), dried over MgSO_4 and concentrated under vacuum. The crude product was purified by chromatography on silica gel to afford amide derivatives.

4.2.5.1. 5-Hydroxy-*N,N*-dimethyl-quinoline-3-carboxamide (**8a**)

Pale yellow solid, yield: 61%. Mp 172°C. R_f = 0.17 (EtOAc). ^1H NMR (300 MHz, $\text{DMSO}-d_6$) δ 10.69 (s, 1H), 8.86 (d, J = 2.1 Hz, 1H), 8.50 (d, J = 2.1 Hz, 1H), 7.62 (t, J = 8.1 Hz, 1H), 7.50 (d, J = 8.7 Hz, 1H), 6.98 (d, J = 8.1 Hz, 1H), 3.03 (br s, 6H) ppm. ^{13}C NMR (75 MHz, $\text{DMSO}-d_6$) δ 168.0, 153.7, 148.6, 148.5, 131.1, 129.2, 127.8, 119.0, 118.0, 109.1, 34.9 ppm. HRMS (ESI+) mass calcd for $[\text{M}+\text{H}]^+$ $\text{C}_{12}\text{H}_{13}\text{N}_2\text{O}_2$ m/z 217.0977, found 217.0971.

4.2.5.2. 5-Hydroxy-*N,N*,4-trimethyl-quinoline-3-carboxamide (**8b**)

White solid, yield: 67%. R_f = 0.06 (EtOAc). Mp 241°C. ^1H NMR (300 MHz, DMSO- d_6) δ 10.45 (s, 1H), 8.48 (s, 1H), 7.52 (t, J = 8.1 Hz, 1H), 7.43 (dd, J = 8.4 Hz, J = 1.2 Hz, 1H), 6.96 (dd, J = 7.5 Hz, J = 1.2 Hz, 1H), 3.06 (s, 3H), 2.80 (s, 3H), 2.74 (s, 3H) ppm. ^{13}C NMR (75 MHz, DMSO- d_6) δ 168.5, 156.1, 149.4, 147.1, 140.8, 130.0, 129.8, 120.1, 118.5, 110.6, 37.7, 34.1, 19.7 ppm. HRMS (ESI+) mass calcd for $[\text{M}+\text{H}]^+$ $\text{C}_{13}\text{H}_{15}\text{N}_2\text{O}_2$ m/z 231.1133, found 231.1135.

4.2.5.3. 5-Hydroxy-*N*-isopropyl-quinoline-3-carboxamide (**8e**)

Pale yellow solid, yield: 70%. R_f = 0.1 (EtOAc). Mp >260°C. ^1H NMR (300 MHz, DMSO- d_6) δ 10.81 (br s, 1H), 9.22 (d, J = 2.4 Hz, 1H), 8.99 (d, J = 2.1 Hz, 1H), 8.66 (d, J = 7.8 Hz, 1H), 7.63 (t, J = 7.8 Hz, 1H), 7.50 (d, J = 8.4 Hz, 1H), 6.99 (d, J = 7.5 Hz, 1H), 4.17 (dq, J = 13.5 Hz, J = 6.7 Hz, 1H), 1.21 (d, J = 6.6 Hz, 6H) ppm. ^{13}C NMR (75 MHz, DMSO- d_6) δ 164.0, 154.3, 149.5, 149.2, 131.6, 130.0, 125.8, 119.0, 118.2, 109.1, 41.1, 22.3 ppm. HRMS (ESI+) mass calcd for $[\text{M}+\text{H}]^+$ $\text{C}_{13}\text{H}_{15}\text{N}_2\text{O}_2$ m/z 231.1133, found 231.1129.

4.2.5.4. 5-Hydroxy-*N*-(2-methoxyethyl)quinoline-3-carboxamide (**8f**)

Pale white solid, yield: 72%. R_f = 0.12 (EtOAc). Mp 198°C. ^1H NMR (300 MHz, DMSO- d_6) δ 10.79 (s, 1H), 9.23 (d, J = 2.4 Hz, 1H), 8.99 (d, J = 1.8 Hz, 1H), 8.93 (br s, 1H), 7.64 (t, J = 8.1 Hz, 1H), 7.49 (d, J = 8.4 Hz, 1H), 6.99 (d, J = 7.5 Hz, 1H), 3.55-3.46 (m, 4H), 3.29 (s, 3H) ppm. ^{13}C NMR (75 MHz, DMSO- d_6) δ 164.9, 154.2, 149.5, 148.9, 131.6, 130.1, 125.3, 119.0, 118.1, 109.1, 70.3, 57.8, 39.4 ppm. HRMS (ESI+) mass calcd for $[\text{M}+\text{H}]^+$ $\text{C}_{13}\text{H}_{15}\text{N}_2\text{O}_3$ m/z 247.1082, found 247.1070.

4.2.5.4. 5-Hydroxy-N-phenyl-quinoline-3-carboxamide (**8g**)

Yellow solid, yield: 71%. R_f = 0.29 (Petroleum Ether:EtOAc 1:2). Mp > 260°C. ^1H NMR (300 MHz, MeOD) δ 9.30-9.29 (m, 2H), 7.76-7.69 (m, 3H), 7.56 (d, J = 8.7 Hz, 1H), 7.42-7.39 (m, 2H), 7.18 (d, J = 7.5 Hz, 1H), 7.02 (d, J = 7.1 Hz, 1H) ppm. ^{13}C NMR (75 MHz, DMSO- d_6) δ 164.1, 154.3, 149.6, 149.2, 139.0, 132.0, 130.7, 128.6, 125.9, 123.8, 120.4, 119.0, 118.1, 109.3 ppm. HRMS (ESI+) mass calcd for $[\text{M}+\text{H}]^+$ $\text{C}_{16}\text{H}_{13}\text{N}_2\text{O}_2$ m/z 265.0977, found 265.0965.

4.2.5.5. Methyl 2-[(5-hydroxyquinoline-3-carbonyl)amino]acetate (**8h**)

White solid, yield: 72%. R_f = 0.28 (EtOAc). Mp 224°C. ^1H NMR (300 MHz, MeOD) δ 9.22 (d, J = 2.1 Hz, 1H), 9.19 (d, J = 1.8 Hz, 1H), 7.70 (t, J = 8.4 Hz, 1H), 7.57 (d, J = 8.4 Hz, 1H), 7.01 (d, J = 7.5 Hz, 1H), 4.21 (s, 2H), 3.79 (s, 3H) ppm. ^{13}C NMR (75 MHz, MeOD) δ 171.8, 168.4, 156.0, 150.7, 149.6, 133.8, 133.1, 126.3, 120.2, 119.5, 110.5, 52.7, 42.3 ppm. HRMS (ESI+) mass calcd for $[\text{M}+\text{H}]^+$ $\text{C}_{13}\text{H}_{13}\text{N}_2\text{O}_4$ m/z 261.0875, found 261.0882.

4.2.5.6. N-Cyclohexyl-5-hydroxy-quinoline-3-carboxamide (**8i**)

Pale yellow solid, yield: 67%. R_f = 0.42 (EtOAc). Mp > 260°C. ^1H NMR (300 MHz, MeOD) δ 9.16 (d, J = 2.1 Hz, 1H), 9.10 (d, J = 2.4 Hz, 1H), 7.66 (t, J = 8.4 Hz, 1H), 7.53 (d, J = 8.4 Hz, 1H), 6.98 (d, J = 7.5 Hz, 1H), 3.98-3.88 (m, 1H), 2.05-1.96 (m, 2H), 1.90-1.81 (m, 2H), 1.77-1.66 (m, 1H), 1.48-1.23 (m, 5H) ppm. ^{13}C NMR (75 MHz, MeOD) δ 167.3, 155.9, 150.4, 149.7, 133.4, 132.8, 127.4, 120.2, 119.4, 110.4, 50.8, 33.7, 26.6, 26.4 ppm. HRMS (ESI+) mass calcd for $[\text{M}+\text{H}]^+$ $\text{C}_{16}\text{H}_{19}\text{N}_2\text{O}_2$ m/z 271.1446, found 271.1434.

4.2.5.8. 5-Hydroxy-N-methyl-quinoline-3-carboxamide (**8j**)

Yellow solid, yield: 79%. Mp 200°C (dec.). R_f = 0.16 (EtOAc). ^1H NMR (300 MHz, MeOD) δ 9.18 (d, J = 2.4 Hz, 1H), 9.12 (d, J = 2.1 Hz, 1H), 7.66 (t, J = 8.4 Hz, 1H), 7.53 (d, J = 8.7, 1H), 6.98 (d, J = 7.5 Hz, 1H), 2.98 (s, 3H). ^{13}C NMR (75 MHz, MeOD) δ 168.5, 155.9, 150.4, 149.5, 133.5, 132.7, 126.7, 120.2, 119.4, 110.4, 27.0 ppm. HRMS (ESI+) mass calcd for $[\text{M}+\text{H}]^+$ $\text{C}_{11}\text{H}_{11}\text{N}_2\text{O}_2$ m/z 203.0820, found 203.0821.

4.2.5.9. 5-hydroxy-N-(2-(2-hydroxyethoxy)ethyl)quinoline-3-carboxamide (**8k**)

Brown solid, yield: 74%. Mp 158-161°C. R_f = 0.05 (EtOAc). ^1H NMR (300 MHz, DMSO- d_6) δ 10.81 (s, 1H), 9.23 (d, J = 2.3 Hz, 1H), 8.99 (s, 1H), 8.92 (s, 1H), 7.69-7.57 (m, 1H), 7.50 (d, J = 8.5 Hz, 1H), 6.99 (d, J = 7.5 Hz, 1H), 4.61 (t, J = 5.2 Hz, 1H), 3.58 (d, J = 5.4 Hz, 2H), 3.54-3.43 (m, 6H). ^{13}C NMR (75 MHz, DMSO- d_6) δ 165.1, 154.3, 149.6, 149.1, 131.8, 130.2, 125.5, 119.1, 118.3, 109.2, 72.2, 68.9, 60.3, 39.4 ppm. HRMS (ESI+) mass calcd for $[\text{M}+\text{H}]^+$ $\text{C}_{14}\text{H}_{17}\text{N}_2\text{O}_4$ m/z 277.1188, found 277.1188.

4.2.6. General procedure for carbamylation of compounds **8a-k**

To a solution of hydroxyquinoline **8a-k** (1.0 mmol) and solid K_2CO_3 (3.0 mmol) in anhydrous DMF (5 mL) was slowly added the corresponding carbamoyl chloride (1.1 mmol) and the mixture was stirred at room temperature. After completion of the reaction, a saturated aqueous solution of ammonium chloride (5 mL) was added and the mixture was extracted with EtOAc (5x5 mL). The combined organic phases were washed with water and brine, dried over MgSO_4 and concentrated under vacuum. The residue was purified by flash chromatography on silica gel to afford the desired carbamylated quinolines **9a-m**.

4.2.6.1. 3-(Dimethylcarbamoyl)-5-quinolyl] *N,N*-dimethylcarbamate (**9a**)

Viscous oil, yield: 85%. R_f = 0.05 (EtOAc). ^1H NMR (300 MHz, CDCl_3) δ 8.93 (d, J = 2.1 Hz, 1H), 8.36 (d, J = 1.5 Hz, 1H), 7.97 (d, J = 8.7 Hz, 1H), 7.72 (t, J = 7.8 Hz, 1H), 7.37 (d, J = 7.5 Hz, 1H), 3.21 (s, 3H), 3.15 (s, 3H), 3.03 (s, 6H) ppm. ^{13}C NMR (75 MHz, CDCl_3) δ 169.0, 154.3, 148.7, 148.5, 147.2, 130.2, 129.9, 129.2, 126.6, 121.9, 119.5, 39.7, 37.0, 36.7, 35.6 ppm. HRMS (ESI+) mass calcd for $[\text{M}+\text{H}]^+$ $\text{C}_{15}\text{H}_{18}\text{N}_3\text{O}_3$ m/z 288.1348, found 288.1340.

4.2.6.2. [3-(Dimethylcarbamoyl)-4-methyl-5-quinolyl] *N,N*-dimethylcarbamate (**9b**)

White solid, yield: 85%. R_f = 0.06 (EtOAc). Mp > 260°C. ^1H NMR (300 MHz, CDCl_3) δ 8.63 (br s, 1H), 7.97 (d, J = 8.4 Hz, 1H), 7.65 (t, J = 7.8 Hz, 1H), 7.21 (d, J = 7.5 Hz, 1H), 3.16 (s, 6H), 3.03 (s, 3H), 2.83 (s, 3H), 2.68 (s, 3H) ppm. ^{13}C NMR (75 MHz, CDCl_3) δ 169.2, 154.9, 149.3, 148.2, 147.4, 139.6, 131.2, 129.1, 128.1, 122.6, 121.7, 38.5, 37.0, 36.6, 34.8, 18.7 ppm. HRMS (ESI+) mass calcd for $[\text{M}+\text{H}]^+$ $\text{C}_{16}\text{H}_{20}\text{N}_3\text{O}_3$ m/z 302.1504, found 302.1495.

4.2.6.3. [3-(Dimethylcarbamoyl)-2-methyl-5-quinolyl] *N,N*-dimethylcarbamate (**9c**)

Pale yellow solid, yield: 86%. R_f = 0.08 (EtOAc). Mp 126°C. ^1H NMR (300 MHz, CDCl_3) δ 8.00 (br s, 1H), 7.79 (d, J = 8.4 Hz, 1H), 7.59 (t, J = 8.4 Hz, 1H), 7.23 (d, J = 8.4 Hz, 1H), 3.10 (s, 3H), 3.07 (s, 3H), 2.94 (s, 3H), 2.75 (s, 3H), 2.59 (s, 3H) ppm. ^{13}C NMR (75 MHz, CDCl_3) δ 169.4, 154.9, 154.0, 148.0, 146.8, 130.3, 129.5, 127.7, 125.6, 120.3, 118.4, 38.4, 36.7, 36.5, 34.6, 22.8 ppm. HRMS (ESI+) mass calcd for $[\text{M}+\text{H}]^+$ $\text{C}_{16}\text{H}_{20}\text{N}_3\text{O}_3$ m/z 302.1504, found 302.1501.

4.2.6.4. [3-(Dimethylcarbamoyl)-2,4-dimethyl-5-quinolyl] *N,N*-dimethylcarbamate (**9d**)

Viscous, colorless oil, yield: 82%. $R_f = 0.1$ (EtOAc). ^1H NMR (300 MHz, CDCl_3) δ 7.91 (d, $J = 4.8$ Hz, 1H), 7.63 (t, $J = 7.8$ Hz, 1H), 7.16 (dd, $J = 7.5$ Hz, $J = 0.9$ Hz, 1H), 3.20 (s, 3H), 3.18 (s, 3H), 3.06 (s, 3H), 2.81 (s, 3H), 2.65 (s, 3H), 2.60 (s, 3H) ppm. ^{13}C NMR (75 MHz, CDCl_3) δ 169.5, 154.6, 154.1, 148.5, 147.8, 138.6, 131.2, 128.6, 127.0, 120.7, 120.5, 37.4, 36.7, 36.3, 34.2, 22.8, 18.4 ppm. HRMS (ESI+) mass calcd for $[\text{M}+\text{H}]^+$ $\text{C}_{17}\text{H}_{22}\text{N}_3\text{O}_3$ m/z 316.1661, found 316.1650.

4.2.6.5. [3-(Isopropylcarbamoyl)-5-quinolyl] *N,N*-dimethylcarbamate (**9e**)

White solid, yield: 76%. $R_f = 0.21$ (EtOAc). Mp $< 50^\circ\text{C}$. ^1H NMR (300 MHz, CDCl_3) δ 9.15 (d, $J = 2.1$ Hz, 1H), 8.72 (dd, $J = 2.1$ Hz, $J = 0.9$ Hz, 1H), 8.01 (dd, $J = 8.7$ Hz, $J = 0.9$ Hz, 1H), 7.76 (dd, $J = 8.4$ Hz, $J = 7.8$ Hz, 1H), 7.39 (dd, $J = 7.5$ Hz, $J = 0.9$ Hz, 1H), 6.06 (br d, $J = 7.5$ Hz, 1H), 4.35 (dq, $J = 13.6$ Hz, $J = 6.6$ Hz, 1H), 3.26 (s, 3H), 3.07 (s, 3H), 1.32 (s, $J = 6.6$ Hz, 6H) ppm. ^{13}C NMR (75 MHz, CDCl_3) δ 164.8, 154.9, 149.5, 148.2, 147.5, 130.5, 130.2, 127.6, 126.5, 121.7, 119.5, 42.4, 37.0, 36.8, 22.8 ppm. HRMS (ESI+) mass calcd for $[\text{M}+\text{H}]^+$ $\text{C}_{16}\text{H}_{20}\text{N}_3\text{O}_3$ m/z 302.1504, found 302.1490.

4.2.6.6. [3-(Isopropylcarbamoyl)-5-quinolyl] *N*-ethyl-*N*-methyl-carbamate (**9f**)

White solid, yield: 73%. Mp 110°C . $R_f = 0.1$ (EtOAc). ^1H NMR of the mixture of two rotamers (300 MHz, CDCl_3) δ 9.10 (s, 1H), 8.61 (s, 0.5H), 8.60 (s, 0.5H), 7.86 (d, $J = 8.4$ Hz, 1H), 7.67-7.61 (m, 1H), 7.31 (d, $J = 7.8$ Hz, 0.5H), 7.27 (d, $J = 8.7$ Hz, 0.5H), 6.71 (br t, $J = 7.2$ Hz, 1H), 4.32-4.21 (m, 1H), 3.55 (q, $J = 7.2$ Hz, 1H), 3.38 (q, $J = 7.2$ Hz, 1H), 3.17 (s, 1.5H), 2.97 (s, 1.5H), 1.31 (t, $J = 7.2$ Hz, 1.5H) 1.22 (d, $J = 6.6$ Hz, 6H), 1.19 (t, $J = 6.9$ Hz, 1.5H) ppm. ^{13}C NMR of the mixture of two rotamers (75. MHz, CDCl_3) δ 164.8, 154.1, 153.9, 149.3, 148.4, 148.2, 147.4, 130.4, 130.2, 129.9, 127.5, 126.4, 126.3, 121.5, 119.3, 44.3,

42.2, 34.5, 34.1, 22.7, 13.5, 12.5 ppm. HRMS (ESI+) mass calcd for $[M+H]^+$ $C_{17}H_{22}N_3O_3$ m/z 316.1661, found 316.1654.

4.2.6.7. [3-(Isopropylcarbamoyl)-5-quinolyl] pyrrolidine-1-carboxylate (**9g**)

Viscous colorless oil, yield: 71%. R_f = 0.23 (EtOAc). 1H NMR (300 MHz, $CDCl_3$) δ 9.14 (d, J = 2.1 Hz, 1H), 8.78 (d, J = 2.1 Hz, 1H), 7.99 (d, J = 8.4 Hz, 1H), 7.77 (t, J = 7.8 Hz, 1H), 7.46 (d, J = 7.5 Hz, 1H), 6.09 (br d, J = 7.8 Hz, 1H), 4.38-4.31 (m, 1H), 3.75 (t, J = 6.6 Hz, 2H), 3.53 (t, J = 6.6 Hz, 2H), 2.07-1.96 (m, 4H), 1.32 (d, J = 6.6 Hz, 6H) ppm. ^{13}C NMR (75 MHz, $CDCl_3$) δ 164.8, 152.5, 149.3, 148.2, 147.3, 130.5, 130.4, 127.5, 126.1, 121.5, 119.3, 46.7, 46.6, 42.2, 25.8, 24.9, 22.6 ppm. HRMS (ESI+) mass calcd for $[M+H]^+$ $C_{18}H_{22}N_3O_3$ m/z 328.1661, found 328.1662.

4.2.6.8. [3-(2-Methoxyethylcarbamoyl)-5-quinolyl] *N,N*-dimethylcarbamate (**9h**)

White solid, yield: 70%. R_f = 0.06 (EtOAc). Mp 138°C. 1H NMR (300 MHz, $CDCl_3$) δ 9.19 (d, J = 1.8 Hz, 1H), 8.69 (d, J = 1.8 Hz, 1H), 7.96 (d, J = 8.4 Hz, 1H), 7.72 (t, J = 7.8 Hz, 1H), 7.36 (d, J = 7.8 Hz, 1H), 6.97 (br s, 1H), 3.69-3.64 (m, 2H), 3.57-3.53 (m, 2H), 3.36 (s, 3H), 3.21 (s, 3H), 3.02 (s, 3H) ppm. ^{13}C NMR (75 MHz, $CDCl_3$) δ 165.6, 154.4, 149.7, 148.2, 147.6, 130.8, 130.4, 127.2, 126.6, 121.8, 119.7, 71.1, 59.0, 40.0, 37.1, 36.8 ppm. HRMS (ESI+) mass calcd for $[M+H]^+$ $C_{16}H_{20}N_3O_4$ m/z 318.1453, found 318.1444.

4.2.6.9. [3-(Phenylcarbamoyl)-5-quinolyl] *N,N*-dimethylcarbamate (**9i**)

Pale yellow solid, yield: 90%. R_f = 0.25 (Petroleum Ether:EtOAc 2:1). Mp 205°C. 1H NMR (300 MHz, acetone- d_6) δ 9.99 (br s, 1H), 9.41 (d, J = 1.8 Hz, 1H), 8.93 (d, J = 1.8 Hz, 1H),

8.00 (d, $J = 8.7$ Hz, 1H), 7.89-7.83 (m, 3H), 7.49 (d, $J = 7.2$ Hz, 1H), 7.42-7.37 (m, 2H), 7.16 (t, $J = 7.5$ Hz, 1H), 3.31 (s, 3H), 3.04 (s, 3H) ppm. ^{13}C NMR (75 MHz, acetone- d_6) δ 164.9, 154.8, 150.4, 150.1, 148.8, 140.0, 131.4, 130.6, 129.6, 129.0, 127.0, 124.9, 122.3, 121.0, 120.4, 37.0, 36.8 ppm. HRMS (ESI+) mass calcd for $[\text{M}+\text{H}]^+$ $\text{C}_{19}\text{H}_{18}\text{N}_3\text{O}_3$ m/z 336.1348, found 336.1347.

4.2.6.10. Methyl 2-[[5-(dimethylcarbamoyloxy)quinoline-3-carbonyl]amino]acetate (**9j**)

White solid, yield: 82%. $R_f = 0.05$ (EtOAc). Mp 141°C. ^1H NMR (300 MHz, CDCl_3) δ 9.27 (d, $J = 2.4$ Hz, 1H), 8.76 (d, $J = 1.8$ Hz, 1H), 8.02 (d, $J = 8.7$ Hz, 1H), 7.80 (t, $J = 7.8$ Hz, 1H), 7.42 (d, $J = 7.8$ Hz, 1H), 6.89 (br s, 1H), 4.32 (d, $J = 7.8$ Hz, 2H), 3.84 (s, 3H), 3.28 (s, 3H), 3.08 (s, 3H) ppm. ^{13}C NMR (75 MHz, CD_3CN) δ 171.0, 166.6, 155.1, 150.2, 149.9, 148.7, 131.7, 130.3, 127.2, 126.9, 122.2, 120.6, 52.6, 42.0, 37.0, 36.9 ppm. HRMS (ESI+) mass calcd for $[\text{M}+\text{H}]^+$ $\text{C}_{16}\text{H}_{18}\text{N}_3\text{O}_5$ m/z 332.1246, found 332.1234.

4.2.6.11. [3-(Cyclohexylcarbamoyl)-5-quinolyl] *N,N*-dimethylcarbamate (**9k**)

Pale yellow solid, yield: 87%. $R_f = 0.36$ (EtOAc). Mp 204°C. ^1H NMR (300 MHz, CDCl_3) δ 9.16 (d, $J = 2.1$ Hz, 1H), 8.72 (d, $J = 1.5$ Hz, 1H), 8.01 (d, $J = 8.7$ Hz, 1H), 7.77 (t, $J = 7.8$ Hz, 1H), 7.40 (d, $J = 7.8$ Hz, 1H), 6.18 (d, $J = 7.2$ Hz, 1H), 4.10-3.95 (m, 1H), 3.27 (s, 3H), 3.07 (s, 3H), 2.14-1.93 (m, 2H), 1.86-1.69 (m, 3H), 1.48-1.21 (m, 5H) ppm. ^{13}C NMR (75 MHz, CDCl_3) δ 164.7, 154.3, 149.2, 148.3, 147.4, 130.4, 130.1, 127.7, 126.3, 121.5, 119.4, 49.2, 36.9, 36.7, 33.0, 25.5, 25.0 ppm. HRMS (ESI+) mass calcd for $[\text{M}+\text{H}]^+$ $\text{C}_{19}\text{H}_{24}\text{N}_3\text{O}_3$ m/z 342.1817, found 342.1810.

4.2.6.12. [3-(Methylcarbamoyl)-5-quinolyl] *N,N*-dimethylcarbamate (**9l**)

Pale yellow solid, yield: 89%. R_f = 0.06 (EtOAc). Mp 182°C. ^1H NMR (300 MHz, CDCl_3) δ 9.18 (d, J = 2.1 Hz, 1H), 8.72 (d, J = 1.5 Hz, 1H), 8.01 (d, J = 8.7 Hz, 1H), 7.77 (t, J = 8.4 Hz, 1H), 7.40 (dd, J = 8.4 Hz, J = 0.9 Hz, 1H), 6.56 (br s, 1H), 3.26 (s, 3H), 3.08 (s, 3H), 3.05 (d, J = 4.8 Hz, 3H) ppm. ^{13}C NMR (75 MHz, CDCl_3) δ 166.0, 154.5, 148.9, 148.4, 147.3, 130.3, 130.0, 127.1, 126.1, 121.5, 119.3, 36.8, 36.5, 26.7 ppm. HRMS (ESI+) mass calcd for $[\text{M}+\text{H}]^+$ $\text{C}_{14}\text{H}_{16}\text{N}_3\text{O}_3$ m/z 274.1191, found 274.1189.

4.2.6.13. 3-((2-(2-hydroxyethoxy)ethyl)carbamoyl)quinolin-5-yl dimethylcarbamate (**9m**)

White solid, yield: 90%. R_f = 0.06 (EtOAc). Mp 104-106°C. ^1H NMR (300 MHz, CDCl_3) δ 9.22 (d, J = 2.1 Hz, 1H), 8.66 (d, J = 1.9 Hz, 1H), 7.96 (br s, 1H), 7.91 (d, J = 8.5 Hz, 1H), 7.68 (appt, J = 8.1 Hz, 1H), 7.31 (d, J = 7.6 Hz, 1H), 3.69-3.64 (m, 2H), 3.64-3.58 (m, 4H), 3.56-3.50 (m, 2H), 3.18 (s, 3H), 2.99 (s, 3H), 2.43 (1H) ppm. ^{13}C NMR (75 MHz, CDCl_3) δ 166.0, 154.7, 149.4, 148.9, 147.6, 130.6, 130.4, 127.5, 126.5, 121.8, 119.6, 72.4, 69.7, 61.6, 40.2, 37.0, 36.8 ppm. HRMS (ESI+) mass calcd for $[\text{M}+\text{H}]^+$ $\text{C}_{17}\text{H}_{22}\text{N}_3\text{O}_5$ m/z 348.1559, found 348.1558.

4.2.7. General procedure for quaternarization of compounds **9a-n,p**

To a stirred solution of carbamylated quinoline **9a-m** (1.0 mmol) in acetonitrile (2 mL) was added methyl iodide or dimethylsulfate (10.0 mmol) (or ethyl iodide (2.0 mmol), or benzyl bromide (1.5 mmol)) at room temperature. The resulting mixture was stirred for 17h at 80°C in sealed tube. After cooling at room temperature, diethylether was added to the mixture and the resulting precipitate was filtered off, rinsed with diethylether and dried under vacuum to afford the corresponding quinolinium salt **2a-n,p**.

4.2.7.1. [3-(Dimethylcarbamoyl)-1-methyl-quinolin-1-ium-5-yl] *N,N*-dimethylcarbamate iodide (**2a**)

Red solid, yield: 94%. Mp 222°C (dec.). ¹H NMR (300 MHz, CDCl₃) δ 10.00 (s, 1H), 9.00 (s, 1H), 8.30 (d, *J* = 8.7 Hz, 1H), 8.20 (t, *J* = 8.7 Hz, 1H), 7.76 (d, *J* = 7.5 Hz, 1H), 4.82 (s, 3H), 3.25 (s, 3H), 3.23 (s, 3H), 3.10 (s, 3H), 3.02 (s, 3H) ppm. ¹³C NMR (75 MHz, CDCl₃) δ 164.0, 152.9, 149.3, 148.8, 139.3, 138.8, 137.0, 130.2, 123.9, 122.9, 115.9, 47.9, 41.1, 37.2, 37.1, 36.0 ppm. HRMS (ESI+) mass calcd for [M]⁺ C₁₆H₂₀N₃O₃, *m/z* 302.1504, found 302.1502.

4.2.7.2. [3-(Dimethylcarbamoyl)-1,2-dimethyl-quinolin-1-ium-5-yl] *N,N*-dimethylcarbamate iodide (**2b**)

Red viscous oil, yield: 93%. ¹H NMR (300 MHz, CDCl₃) δ 8.71 (s, 1H), 8.17-8.07 (m, 2H), 7.76 (dd, *J* = 6.9 Hz, *J* = 4.5 Hz, 1H), 4.66 (s, 3H), 3.26 (s, 6H), 3.25 (s, 3H), 3.23 (s, 3H), 3.10 (s, 3H) ppm. ¹³C NMR (75 MHz, CDCl₃) δ 165.3, 158.7, 153.0, 148.6, 140.2, 136.7, 136.4, 133.2, 122.7, 122.0, 115.8, 42.9, 40.9, 37.3, 37.1, 35.5, 22.6 ppm. HRMS (ESI+) mass calcd for [M]⁺ C₁₇H₂₂N₃O₃, *m/z* 316.1661, found 316.1668.

4.2.7.3. [3-(Dimethylcarbamoyl)-1,4-dimethyl-quinolin-1-ium-5-yl] *N,N*-dimethylcarbamate iodide (**2c**)

Red viscous oil, yield: 94%. ¹H NMR (300 MHz, CDCl₃) δ 9.62 (s, 1H), 8.16-8.07 (m, 2H), 7.63 (dd, *J* = 7.2 Hz, *J* = 1.5 Hz, 1H), 4.74 (s, 3H), 3.24 (s, 3H), 3.21 (s, 6H), 3.10 (s, 3H), 2.96 (s, 3H) ppm. ¹³C NMR (75 MHz, CDCl₃) δ 164.2, 153.5, 153.4, 150.4, 147.3, 139.0,

135.8, 132.4, 125.5, 124.7, 116.9, 48.2, 40.2, 37.4, 37.1, 35.5, 20.9 ppm. HRMS (ESI+) mass calcd for $[M]^+ C_{17}H_{22}N_3O_3$, m/z 316.1661, found 316.1662.

4.2.7.4. [3-(Dimethylcarbamoyl)-1,2,4-trimethyl-quinolin-1-ium-5-yl] *N,N*-dimethylcarbamate iodide (**2d**)

Orange oil, yield: 92%. Mp 159°C. 1H NMR (300 MHz, $CDCl_3$) δ 8.16-8.03 (m, 2H), 7.55 (dd, $J = 7.5$ Hz, $J = 1.2$ Hz, 1H), 4.61 (s, 3H), 3.23 (s, 6H), 3.20 (s, 3H), 3.17 (s, 3H), 3.09 (s, 3H), 2.88 (s, 3H) ppm. ^{13}C NMR (75 MHz, $CDCl_3$) δ 165.6, 156.6, 153.5, 151.1, 150.0, 140.2, 135.2, 134.4, 124.5, 123.2, 117.1, 43.2, 39.8, 37.2, 36.9, 35.0, 22.9, 20.9 ppm. HRMS (ESI+) mass calcd for $[M]^+ C_{18}H_{24}N_3O_3$, m/z 330.1817, found 330.1816.

4.2.7.5. [3-(Isopropylcarbamoyl)-1-methyl-quinolin-1-ium-5-yl] *N,N*-dimethylcarbamate iodide (**2e**)

Yellow solid, yield: 99%. Mp 232°C. 1H NMR (300 MHz, $CDCl_3$) δ 11.0 (s, 1H), 9.65 (s, 1H), 8.82 (d, $J = 7.2$ Hz, 1H), 8.23 (t, $J = 8.1$ Hz, 1H), 8.07 (d, $J = 8.7$ Hz, 1H), 7.86 (d, $J = 7.8$ Hz, 1H), 4.83 (s, 3H), 4.46-4.39 (m, 1H), 3.29 (s, 3H), 3.09 (s, 3H), 1.45 (d, $J = 6.6$ Hz, 6H) ppm. ^{13}C NMR (75 MHz, $DMSO-d_6$) δ 160.3, 152.8, 149.5, 148.1, 142.1, 139.1, 137.4, 128.4, 124.0, 122.9, 115.1, 46.9, 43.7, 37.3, 37.1, 22.5 ppm. HRMS (ESI+) mass calcd for $[M]^+ C_{17}H_{22}N_3O_3$, m/z 316.1661, found 316.1651.

4.2.7.6. [3-(Isopropylcarbamoyl)-1-methyl-quinolin-1-ium-5-yl] *N*-ethyl-*N*-methyl-carbamate iodide (**2f**)

Red solid, yield: 99%. Mp 138°C. ^1H NMR of the mixture of two rotamers (300 MHz, CDCl_3) δ 10.97 (s, 0.5H), 10.95 (s, 0.5H), 9.64 (s, 0.5H), 9.63 (s, 0.5H), 8.74 (t, $J = 6.9$ Hz, 1H), 8.27-8.14 (m, 2H), 7.86 (t, $J = 7.8$ Hz, 1H), 4.85 (2s, 3H), 4.46-4.36 (m, 1H), 3.67 (q, $J = 6.9$ Hz, 1H), 3.47 (q, $J = 6.9$ Hz, 1H), 3.26 (s, 1.5H), 3.07 (s, 1.5H), 1.46-1.36 (m, 7.5H), 1.26 (t, $J = 6.9$ Hz, 1.5H) ppm. ^{13}C NMR of the mixture of two rotamers (75 MHz, CDCl_3) δ 160.2, 160.1, 152.3, 152.2, 149.3, 147.9, 141.8, 139.0, 137.4, 128.2, 128.1, 123.8, 123.7, 122.7, 122.6, 115.2, 115.0, 46.9, 44.6, 44.5, 43.4, 34.6, 34.3, 22.3, 13.4, 12.2 ppm. HRMS (ESI+) mass calcd for $[\text{M}]^+ \text{C}_{18}\text{H}_{24}\text{N}_3\text{O}_3$, m/z 330.1817, found 330.1810.

4.2.7.7. [3-(Isopropylcarbamoyl)-1-methyl-quinolin-1-ium-5-yl] pyrrolidine-1-carboxylate iodide (**2g**)

Red solid, yield: 98%. Mp 218°C. ^1H NMR (300 MHz, CDCl_3) δ 11.07 (s, 1H), 9.71 (s, 1H), 8.85 (d, $J = 6.9$ Hz, 1H), 8.23 (t, $J = 8.4$ Hz, 1H), 8.05-7.96 (m, 2H), 4.83 (s, 3H), 4.49-3.38 (m, 1H), 3.79 (t, $J = 6.6$ Hz, 2H), 3.56 (t, $J = 6.6$ Hz, 2H), 2.09-2.00 (m, 4H), 1.47 (d, $J = 6\text{H}$) ppm. ^{13}C NMR (75 MHz, CDCl_3) δ 160.2, 150.6, 149.0, 148.0, 142.1, 141.7, 138.9, 137.4, 127.9, 123.5, 122.4, 114.9, 47.0, 46.9, 46.8, 43.4, 25.5, 24.6, 22.2 ppm. HRMS (ESI+) mass calcd for $[\text{M}]^+ \text{C}_{19}\text{H}_{24}\text{N}_3\text{O}_3$, m/z 342.1818, found 342.1819.

4.2.7.8. [3-(2-Methoxyethylcarbamoyl)-1-methyl-quinolin-1-ium-5-yl] *N,N*-dimethylcarbamate iodide (**2h**)

Yellow solid, yield: 92%. Mp 120°C. ^1H NMR (300 MHz, CDCl_3) δ 11.0 (s, 1H), 9.69 (s, 1H), 9.02 (br s, 1H), 8.24 (t, $J = 8.7$ Hz, 1H), 8.16 (d, $J = 8.7$ Hz, 1H), 7.86 (d, $J = 7.8$ Hz, 1H), 4.82 (s, 3H), 3.75 (br s, 4H), 3.40 (s, 3H), 3.29 (s, 3H), 3.08 (s, 3H) ppm. ^{13}C NMR (75 MHz, CDCl_3) δ 161.5, 152.8, 149.7, 148.5, 142.0, 139.2, 137.6, 128.1, 124.0, 123.0, 114.8,

70.3, 58.8, 46.9, 40.1, 37.3, 37.2 ppm. HRMS (ESI+) mass calcd for $[M]^+$ $C_{17}H_{22}N_3O_4$, m/z 332.1610, found 332.1611.

4.2.7.9. *[1-Methyl-3-(phenylcarbamoyl)quinolin-1-ium-5-yl] N,N-dimethylcarbamate iodide (2i)*

Orange solid, yield: 96%. Mp 152°C. 1H NMR (300 MHz, CD_2Cl_2) δ 10.54 (s, 1H), 10.45 (s, 1H), 9.61 (s, 1H), 8.10 (t, $J = 8.4$ Hz, 1H), 7.92-7.84 (m, 3H), 7.74 (d, $J = 7.8$ Hz, 1H), 7.17 (t, $J = 7.8$ Hz, 1H), 7.00 (t, $J = 7.2$ Hz, 1H), 4.60 (s, 3H), 3.20 (s, 3H), 2.96 (s, 3H) ppm. ^{13}C NMR (75 MHz, CD_2Cl_2) δ 160.2, 153.1, 150.1, 149.1, 142.6, 139.5, 138.3, 137.8, 129.0, 128.2, 125.3, 124.0, 123.1, 121.1, 114.8, 47.0, 37.4 ppm. HRMS (ESI+) mass calcd for $[M]^+$ $C_{20}H_{20}N_3O_3$, m/z 350.1504, found 350.1504.

4.2.7.10. *Methyl 2-[[5-(dimethylcarbamoyloxy)-1-methyl-quinolin-1-ium-3-carbonyl]amino]acetate iodide (2j)*

Yellow solid, yield: 95%. Mp 240°C (dec.). 1H NMR (300 MHz, $DMSO-d_6$) δ 9.98-9.90 (m, 2H), 9.57 (s, 1H), 8.46-8.35 (m, 2H), 7.95 (d, $J = 8.7$ Hz, 1H), 4.70 (s, 3H), 4.21 (d, $J = 5.7$ Hz, 2H), 3.70 (s, 3H), 3.27 (s, 3H), 3.03 (s, 3H) ppm. ^{13}C NMR (75 MHz, $DMSO-d_6$) δ 169.9, 162.1, 153.0, 150.7, 148.7, 139.2, 138.5, 136.8, 126.5, 123.1, 123.0, 116.3, 52.0, 46.2, 41.4, 36.8, 36.6 ppm. HRMS (ESI+) mass calcd for $[M]^+$ $C_{17}H_{20}N_3O_5$, m/z 346.1403, found 346.1395.

4.2.7.11. *[3-(Cyclohexylcarbamoyl)-1-methyl-quinolin-1-ium-5-yl] N,N-dimethylcarbamate iodide (2k)*

Red solid, yield: 95%. Mp 200°C. ^1H NMR (300 MHz, CDCl_3) δ 10.7 (s, 1H), 9.58 (s, 1H), 8.62 (d, $J = 7.8$ Hz, 1H), 8.21-8.19 (m, 2H), 7.79 (t, $J = 4.2$ Hz, 1H), 4.78 (s, 3H), 4.10-3.94 (m, 1H), 3.25 (s, 3H), 3.03 (s, 3H), 2.04-1.88 (m, 2H), 1.84-1.55 (m, 5H), 1.40-1.13 (m, 3H) ppm. ^{13}C NMR (75 MHz, CDCl_3) δ 160.3, 152.9, 149.5, 148.1, 142.1, 139.1, 137.4, 128.5, 124.0, 122.8, 115.1, 50.9, 47.0, 37.3, 37.0, 32.6, 25.3, 25.2 ppm. HRMS (ESI+) mass calcd for $[\text{M}]^+ \text{C}_{20}\text{H}_{26}\text{N}_3\text{O}_3$, m/z 356.1974, found 356.1970.

4.2.7.12. [1-Methyl-3-(methylcarbamoyl)quinolin-1-ium-5-yl] *N,N*-dimethylcarbamate iodide (2l)

Yellow solid, yield: 99%. Mp 230°C. ^1H NMR (300 MHz, CDCl_3) δ 11.0 (s, 1H), 9.71 (s, 1H), 9.11 (s, 1H), 8.25 (t, $J = 8.7$ Hz, 1H), 8.05 (d, $J = 9.2$ Hz, 1H), 7.88 (d, $J = 8.1$ Hz, 1H), 4.82 (s, 3H), 3.31 (s, 3H), 3.10 (s, 3H), 3.09 (d, $J = 6.0$ Hz, 3H) ppm. ^{13}C NMR (75 MHz, $\text{DMSO}-d_6$) δ 161.8, 152.9, 150.6, 148.6, 138.9, 138.0, 136.5, 127.5, 123.0, 122.9, 116.2, 46.1, 36.8, 36.6, 26.4 ppm. HRMS (ESI+) mass calcd for $[\text{M}]^+ \text{C}_{15}\text{H}_{18}\text{N}_3\text{O}_3$, m/z 288.1348, found 288.1339.

4.2.7.13. [1-Ethyl-3-(methylcarbamoyl)quinolin-1-ium-5-yl] *N,N*-dimethylcarbamate iodide (2m)

Yellow solid, yield: 97%. ^1H NMR (300 MHz, CDCl_3) δ 11.13 (d, $J = 1.8$ Hz, 1H), 9.71 (s, 1H), 9.23 (s, 1H), 8.24 (t, $J = 8.4$ Hz, 1H), 8.05 (d, $J = 9.0$ Hz, 1H), 7.87 (d, $J = 7.8$ Hz, 1H), 5.33 (q, $J = 7.2$ Hz, 2H), 3.32 (s, 3H), 3.11 (s, 3H), 3.10 (d, $J = 6.0$ Hz, 3H), 1.86 (t, $J = 7.2$ Hz, 3H) ppm. ^{13}C NMR (75 MHz, CDCl_3) δ 161.6, 152.8, 150.1, 147.4, 142.2, 138.3, 137.5, 128.7, 124.7, 122.8, 114.6, 54.7, 37.4, 37.2, 26.7, 15.7 ppm. HRMS (ESI+) mass calcd for $[\text{M}]^+ \text{C}_{16}\text{H}_{20}\text{N}_3\text{O}_3$, m/z 302.1505, found 302.1499.

4.2.7.14. [1-Benzyl-3-(methylcarbamoyl)quinolin-1-ium-5-yl] *N,N*-dimethylcarbamate bromide (**2n**)

Red solid, yield: 85%. Mp 210°C. ¹H NMR (300 MHz, CDCl₃) δ 11.35 (s, 1H), 9.76 (s, 1H), 9.74 (br s, 1H), 8.17-8.05 (m, 2H), 7.77 (d, *J* = 7.5 Hz, 1H), 7.34 (br s, 5H), 6.48 (s, 2H), 3.30 (s, 3H), 3.12 (d, *J* = 4.5 Hz, 3H), 3.07 (s, 3H) ppm. ¹³C NMR (75 MHz, CDCl₃) δ 161.5, 152.7, 149.9, 149.3, 142.5, 138.5, 137.1, 131.9, 129.7, 128.6, 127.2, 124.7, 122.6, 115.1, 61.7, 37.3, 37.0, 27.0 ppm. HRMS (ESI+) mass calcd for [M]⁺ C₂₁H₂₂N₃O₃, *m/z* 364.1661, found 364.1660.

4.2.7.15. 5-((dimethylcarbamoyl)oxy)-3-((2-(2-hydroxyethoxy)ethyl)carbamoyl)-1-methylquinolin-1-ium methyl sulfate (**2p**)

White solid, yield: 81%. ¹H NMR (300 MHz, D₂O) δ 9.71 (s, 1H), 9.58 (s, 1H), 8.37-8.35 (m, 2H), 7.89 (d, *J* = 7.4 Hz, 1H), 4.75 (s, 3H), 3.84-3.68 (m, 11H), 3.32 (s, 3H), 3.08 (s, 3H) ppm. ¹³C NMR (75 MHz, CDCl₃) δ 161.8, 153.0, 149.5, 149.3, 141.1, 139.4, 137.3, 128.6, 123.9, 122.8, 115.6, 72.5, 69.0, 61.5, 54.6, 46.9, 40.7, 37.2, 36.9 ppm. HRMS (ESI+) mass calcd for [M]⁺ C₁₈H₂₄N₃O₅, *m/z* 362.1716, found 362.1710.

4.2.8. *N*-{2-(2-(2-(1,3-dioxoisindolin-2-yl)ethoxy)ethoxy)ethyl}-5-hydroxyquinoline-3-carboxamide (**11a**)

N,N'-Carbonyldiimidazole (0.13 g, 0.8 mmol) was added to a solution of acid 5-hydroxyquinoline-3-carboxylic acid **7a** (0.1 g, 0.53 mmol) in DMF (1 mL) under nitrogen and the mixture was stirred at 40°C for 1h. Amine derivative **10**, prepared as described by Pastorin et al.,[35] (0.2 g, 0.53 mmol) and triethylamine (0.22 mL) in DMF (1 mL) were

added and the mixture was stirred at 20°C overnight. Solvent was removed under vacuum and the residue was taken up in CH₂Cl₂, washed successively with water and brine, and then dried over MgSO₄. The organic phase was evaporated and the resulted residue was purified by flash chromatography on silica gel (AcOEt/MeOH = 97:3) to give **11a** as a colourless oil (89.5 mg, 32%). ¹H NMR (300 MHz, CDCl₃) δ 9.37 (d, *J* = 2.2 Hz, 1H), 9.04 (d, *J* = 2.2 Hz, 1H), 7.73 (dd, *J* = 5.4, 3.1 Hz, 2H), 7.67-7.53 (m, 4H), 6.97 (d, *J* = 7.1 Hz, 1H), 3.93 (t, *J* = 5.9 Hz, 2H), 3.79 (t, *J* = 5.8 Hz, 2H), 3.74-3.60 (m, 8H) ppm. ¹³C NMR (75 MHz, CD₃CN) δ 169.5, 167.3, 155.3, 150.7, 150.1, 135.3, 133.2, 133.1, 131.8, 127.0, 124.0, 120.4, 119.9, 110.4, 71.1, 71.0, 70.3, 68.8, 61.2, 40.8, 38.5 ppm. HRMS (ESI+) mass calcd for [M+H]⁺ C₂₄H₂₄N₃O₆, *m/z* 450.1665, found 450.1653.

4.2.9. 3-{(2-(2-(2-(1,3-dioxoisindolin-2-yl)ethoxy)ethoxy)ethyl)carbamoyl}quinolin-5-yl dimethylcarbamate (**11b**)

To a suspension of **11a** (77.3 mg, 0.17 mmol), dry K₂CO₃ (120.1 mg, 0.86 mmol) in dry acetonitrile (10 mL) was added dimethylcarbamoyl chloride (20 mL, 0.22 mmol). Thereafter, the mixture was refluxed for 18h under nitrogen. The solvent was removed under vacuum and the residue taken up in dichloromethane, washed with water, then brine and dried over MgSO₄. The resulting residue was purified by flash chromatography on silica gel (AcOEt/MeOH = 97:3) to give 65.4 mg of **11b** (73%) as a white solid (mp 152-153°C). ¹H NMR (300 MHz, CDCl₃) δ 9.33 (d, *J* = 2.2 Hz, 1H), 8.84-8.74 (m, 1H), 7.95 (d, *J* = 8.5 Hz, 1H), 7.77-7.66 (m, 3H), 7.61 (dd, *J* = 5.6, 3.0 Hz, 2H), 7.54-7.41 (m, 1H), 7.35 (dd, *J* = 7.7, 0.8 Hz, 1H), 3.86 (t, *J* = 5.4 Hz, 2H), 3.72 (t, *J* = 5.4 Hz, 2H), 3.67-3.50 (m, 8H), 3.21 (s, 3H), 3.01 (s, 3H). ¹³C NMR (75 MHz, CDCl₃) δ 168.4, 165.7, 154.4, 149.7, 148.7, 147.7, 134.1,

132.0, 130.6, 127.3, 126.6, 123.2, 121.9, 119.5, 70.3, 69.9, 69.8, 68.04, 40.1, 37.3, 37.0, 36.8.

HRMS (ESI+) mass calcd for $[M+H]^+$ $C_{27}H_{29}N_4O_7$ m/z 521.2036, found 521.2039.

4.2.10. *5-((dimethylcarbamoyl)oxy)-3-((2-(2-(2-(1,3-dioxoisindolin-2-yl)ethoxy)ethoxy)ethyl)carbamoyl)-1-methyl quinolin-1-ium triflate (4)*

To a stirred solution of carbamylated quinoline **11b** (40.0 mg, 0.077 mmol) in dry dichloromethane (2 mL) was added methyl trifluoromethanesulfonate (9.2 mL, 85 mmol) at 20°C. The resulting mixture was stirred for 2h at 20°C after which the solvent was evaporated. Diethyl ether (5 mL) was added and the precipitated formed was collected to afford the quinolinium salt **4** (45.2 mg, 86%) as a light yellow hygroscopic powder. 1H NMR (300 MHz, $CDCl_3$) δ 9.83 (s, 1H), 9.60 (d, J = 1.0 Hz, 1H), 8.53 (s, 1H), 8.20 (d, J = 4.7 Hz, 2H), 7.76 (dq, J = 6.8, 4.2 Hz, 3H), 7.66 (dd, J = 5.6, 3.0 Hz, 2H), 4.72 (s, 3H), 3.82 (t, J = 5.6 Hz, 2H), 3.69 (t, J = 5.6 Hz, 2H), 3.61 (dd, J = 5.2, 3.7 Hz, 8H), 3.26 (s, 3H), 3.04 (s, 3H). ^{13}C NMR (75 MHz, $CDCl_3$) δ 168.4, 161.5, 152.9, 149.6, 149.2, 141.4, 139.4, 137.6, 134.1, 132.0, 128.6, 124.1, 123.3, 122.9, 115.29, 70.1, 70.0, 68.9, 67.9, 46.9, 40.4, 37.4, 37.3, 37.0. HRMS (ESI+) mass calcd for $[M]^+$ $C_{28}H_{31}N_4O_7$ m/z 535.2193, found 535.2195.

4.2.11. *3-((2-(2-(2-(1,3-dioxoisindolin-2-yl)ethoxy)ethoxy)ethyl)carbamoyl)-1-methyl-1,4-dihydroquinolin-5-yl dimethylcarbamate (3)*

To a solution of quinolinium salt **4a** (60.0 mg, 0.087 mmol) in dry degassed acetonitrile (1 mL) was added BNAH (19.0 mg, 1 equiv). The reaction was stirred in the dark for 36h. Then the solvent was removed under reduced pressure and the residue taken-up in dichloromethane. The organic phase was washed with water and brine, dried over $MgSO_4$ and concentrated under *vacuum* to afford the desired dihydroquinoline **3** (41.3 mg, 87%) as an yellow oil. 1H

NMR (300 MHz, CD₃CN) δ 7.82-7.68 (m, 4H), 7.11 (t, J = 8.2 Hz, 1H), 7.01 (s, 1H), 6.63-6.62 (m, 2H), 6.14 (t, J = 5.2 Hz, 1H), 3.79 (dd, J = 8.7, 3.0 Hz, 2H), 3.67 (dd, J = 8.6, 3.0 Hz, 2H), 3.55 (dd, J = 5.9, 2.8 Hz, 2H), 3.49 (dd, J = 5.8, 2.6 Hz, 4H), 3.41 (t, J = 5.7 Hz, 2H), 3.27 (q, J = 5.6 Hz, 2H), 3.15 (s, 3H), 3.06 (s, 3H), 2.92 (s, 3H). ¹³C NMR (75 MHz, CD₃CN) δ 169.2, 167.8, 155.1, 151.3, 141.7, 139.2, 135.1, 133.1, 128.3, 123.1, 117.0, 116.7, 110.3, 100.6, 70.9, 70.8, 70.5, 68.4, 39.8, 39.5, 38.3, 37.0, 36.9, 22.0. HRMS (ESI+) mass calcd for [M+H]⁺ C₂₈H₃₃N₄O₇ m/z 537.2349, found 537.2358.

4.2.12. 3-((2-(2-(2-(1,3-dioxoisindolin-2-yl)ethoxy)ethoxy)ethyl)carbamoyl)-5-hydroxy-1-methylquinolin-1-ium iodide (**12**)

To a solution of compound **11a** (45.0 mg, 0.1 mmol) in dry degassed acetonitrile (1 mL) was added methyl iodide (31.0 μ L, 5 equiv). The reaction was stirred at 40°C for 20h in sealed tube. Then the solvent was removed under reduced pressure and the residue taken-up in diethylether. The resulting precipitate was filtered off and rinsed twice with diethylether. The obtained red solid was dried under *vacuum* to afford the desired quinolinium salt **12** (38.1 mg, 82%) as an red solid. ¹H NMR (300 MHz, CD₃OD) δ 9.75 (s, 1H), 9.62 (s, 1H), 8.10 (t, J = 8.2 Hz, 1H), 7.79-7.768 (m, 5H), 7.24 (d, J = 8.0 Hz, 1H), 4.60 (s, 3H), 3.87-3.83 (m, 2H), 3.77-3.73 (m, 2H), 3.68-3.60 (m, 8H). ¹³C NMR (75 MHz, CD₃OD) δ 169.7, 164.0, 158.7, 150.9, 141.4, 141.3, 140.1, 135.3, 133.2, 127.1, 124.0, 122.3, 113.7, 109.5, 71.3, 71.2, 70.2, 68.9, 46.7, 41.3, 38.3. HRMS (ESI+) mass calcd for [M]⁺ C₂₅H₂₆N₃O₆ m/z 464.1821, found 464.1823.

4.3. Biology

4.3.1. AChE inhibition Assay

Inhibitory capacity of compounds on AChE biological activity was evaluated through the use of the spectrometric method of Ellman. Acetylthiocholine iodide and 5,5-dithiobis-(2-nitrobenzoic) acid (DTNB) were purchased from Sigma Aldrich. AChE from human erythrocytes (buffered aqueous solution, ≥ 500 units/mg protein (BCA), Sigma Aldrich) was diluted in 20 mM HEPES buffer pH 8, 0.1% Triton X-100 such as to have enzyme solution with 0.25 units/mL enzyme activity.

In the procedure, 100 μ L of 0.3 mM DTNB dissolved in phosphate buffer pH 7.4 were added into the 96 wells plate followed by 50 μ L of the tested compound solution and 50 μ L of enzyme solution. After 5 min of preincubation, the reaction was then initiated by the injection of 50 μ L of 10 mM acetylthiocholine iodide solution.

The hydrolysis of acetylthiocholine was monitored by the formation of yellow 5-thio-2-nitrobenzoate anion as the result of the reaction of DTNB with thiocholine, released by the enzymatic hydrolysis of acetylthiocholine, at a wavelength of 412 nm every minute for 10 min using a 96-well microplate plate reader (TECAN Infinite[®] M200, Lyon, France). Tested compounds were dissolved in analytical grade DMSO. Donepezil was used as reference standard. First screening of AChE from human erythrocytes activity were carried out at 10^{-6} M concentration of compounds respectively under study. For the compounds with significant inhibition ($\geq 50\%$) after 4 min of reaction, IC_{50} values were determined graphically from 6 points inhibition curves using the Origin[®] software.

4.3.1.2. Propidium competition assay

Propidium exhibits an increase in fluorescence on binding to AChE peripheral site, making it a useful probe for competitive ligand binding to the enzyme. Fluorescence was measured in a Tecan Infinite[®] M200 plate reader. Measurements were carried out in 200 μ L solution volume, in 96-well plates. The buffer used was 1 mM Tris/HCl, pH 8.0, 5 U EeAChE which was incubated, for 6 hours at 25°C, with a 150 μ L 10^{-5} M solution of the compounds or donepezil (from Tocris) as control. One micromolar propidium iodide 50 μ L solution was added 10 min before fluorescence measurement. The excitation wavelength was 535 nm, and that of emission, 595 nm. Each assay was repeated, at least, at three different times.

4.3.1.3. Inhibition of Self-Induced A β (1–42) Aggregation in the presence of **4**.

The Sensolyte ThT β -amyloid (1–42) aggregation kit provided a convenient and standard method to measure A β (1–42) aggregation using thioflavin T dye. A β (1–42) peptide was pretreated to ensure it was in a monomeric state. An optimized fibrillation buffer was included with the kit, and two known inhibitors were supplied as controls. The protocol used was the one indicated by the supplier (β amyloid aggregation Sensolyte thioflavin kit; Anaspec ref. 72214). Briefly, stock solution of the compound **4** was prepared at a concentration of 1 mM in DMSO. Then, 1 μ L of the solution was placed in a 96-well plate. So, 10 μ L of the thioflavine T solution (2 mM) and 85 μ L of the solution of the amyloid β -peptide 1–42 (250 μ g/mL in the supplied buffer) were added to each well. The reaction volume was made up to 100 μ L with the reaction buffer supplied by the kit. In parallel, a positive control was performed without compound and references were tested (curcumin, 10 μ M / morin and phenol red, 100 μ M). Each compound was tested in triplicate. The fluorescence was measured every 5 min at 37°C ($\lambda_{\text{ex}}/\lambda_{\text{em}} = 440 \text{ nm}/484 \text{ nm}$) with the Infinite[®] M200 reader (Tecan). The calculation of percent inhibition was performed as follows: $100 - (IF_i/IF_0 \times 100)$, with IF_i corresponding to

the fluorescence measured in the presence of the tested compound and IF₀ without the tested compound.

4.3.1.4. Caco-2 (A-B) permeability assay

The Caco-2 (A-B) permeability assay was performed by Cerep, Inc. (Redmond, WA98052, USA). Caco-2 cells were cultured for 25 days to form a monolayer on 96-well multiscreen plates. All samples were run apical (A) side to basolateral (B) side at 37°C with pH 7.4 buffer in both the donor and receiver chambers. The prodrug **3** was added to the donor chamber at 10 µM and samples were analyzed at 0 and 60 min by HPLC-MS/MS. The apparent permeability coefficient (P_{app}) was calculated from the following equation: $P_{app} \text{ (cm/s)} = (V_R \times C_{R,end}/\Delta t) \times (1/(A \times (C_{D,mid} - C_{R,mid})))$. Where V_R is the volume of in the receiver chamber, $C_{R,end}$ is the concentration of compound in the receiver chamber at the end of the time point, Δt is the incubation time (60 min), and A is the surface area of the cell monolayer. $C_{D,mid}$ is the calculated midpoint concentration of the compound in the donor chamber and $C_{R,mid}$ is the midpoint concentration of the test compound in the receiver chamber. Concentration of the compound were expressed as peak areas of the test compound. The recovery of the test compound was calculated as follows: $\text{Recovery (\%)} = (V_D \times C_{D,end} + V_R \times C_{R,end}) \times 100 / (V_D \times C_{D0})$ where V_D and V_R are the volumes of the donor and receiver chambers, respectively. $C_{D,end}$ is the concentration of the test compound in the donor sample at the end time point. $C_{R,end}$ is the concentration of the test compound in the receiver sample at the end time point. C_{D0} is the concentration of the test compound in the donor sample at time zero. Concentrations of the test compound are expressed as peak areas of the test compound.

4.4. Docking simulation

The crystal structures (PDB ID: 2CKM and PDB 4EY7) of the torpedo and human acetylcholine esterase respectively in complex with the alkylene- linked bis-tacrine dimer and donepezil were downloaded from the RCSB Web site (<http://www.pdb.org>). The ligands were drawn in Marvin Sketch [39], hydrogen were added and its energy was minimized with Chimera 1.5.3 software with default setting [40]. Autodock Tools (ADT 1.5.6) was used to add Gasteiger charges to the ligand and to control the flexible torsions [41]. Before the docking, the protein was prepared with the DockPrep module of Chimera 1.5.3 software with default setting. The original crystal ligand and water molecules were removed from the protein–ligand complexes and ADT 1.5.6 was used with the default setting to add polar hydrogens atoms and to assign Kollman charges. The docking studies of compound **2h**, **2j**, **2k**, **2p** or **4** with the *TcAChE* protein and **4** with *rhAChE* protein were carried out using AutodockVina [29] with the docking parameters set at default values. For *TcAChE* prtotein, the box center was set to 4.9799/66.3727/70.6527 and the box size was set to 25 Å in each dimension. For *rhAChE*, the box center was set to -13.8673/-48.5081/34.708 and the box size was set to 25/32/27 Å. Visualization was performed in PyMol 0.99rc6 [30]. The docking procedure were validated by redocking the original ligands into the AChE proteins.

Acknowledgments

This work was partly supported by INSA-Rouen, Rouen University, CNRS, Labex SynOrg (ANR-11-LABX-0029), Région Haute-Normandie.

Conflict of interest

The authors declare no competing financial interest.

Appendix A. Supplementary data

- NMR spectra ($^1\text{H}/^{13}\text{C}$) of compounds **6b**, **7b**, **8b-k**, **9a-m**, **2a-n,p**, **11a-b**, **12**, **4** and **3**.

References

- [1] Alzheimer's Association, 2015 Alzheimer's disease facts and figures, *Alzheimers Dement.* 11 (2015) 332–384.
- [2] E. Scarpini, P. Schelterns, H. Feldman, Treatment of Alzheimer's disease; current status and new perspectives *Lancet Neurol.* 2 (2003) 539-547.
- [3] D. A. Smith, Treatment of Alzheimer's disease in the long-term-care setting, *Am. J. Health Syst. Pharm.* 66 (2009) 899-907.
- [4] F. Ma, H. Du, Novel deoxyvasicinone derivatives as potent multitarget-directed ligands for the treatment of Alzheimer's disease: Design, synthesis, and biological evaluation, *Eur. J. Med. Chem.* 140 (2017) 118-127.
- [5] S.S. Xie, X. Wang, N. Jiang, W. Yu, K.D. Wang, J.S. Lan, Z.R. Li, L.Y. Kong, Multi-target tacrine-coumarin hybrids: Cholinesterase and monoamine oxidase B inhibition properties against Alzheimer's disease, *Eur. J. Med. Chem.* 95 (2015) 153-165.
- [6] J.S. Lan, Y. Ding, Y. Liu, P. Kang, J. W. Hou, X.Y. Zhang, S.S. Xie, T. Zhang, Design, synthesis and biological evaluation of novel coumarin-*N*-benzyl pyridinium hybrids as multi-target agents for the treatment of Alzheimer's disease, *Eur. J. Med. Chem.* 139 (2017) 48-59.
- [7] N. Jiang, Q. Huang, J. Liu, N. Liang, Q. Li, Q. Li, S.S. Xie, Design, synthesis and biological evaluation of new coumarin dithiocarbamate hybrids as multifunctional agents for the treatment of Alzheimer's disease, *Eur. J. Med. Chem.* 146 (2018) 287-298.
- [8] K. Czarnecka, N. Chufarova, K. Halczuk, K. Maciejewska, M. Girek, R. Skibinski, J. Jonczyk, M. Bajda, J. Kabzinski, I. Majsterek, P. Szymanski, Tetrahydroacridine derivatives

with dichloronicotinic acid moiety as attractive, multipotent agents for Alzheimer's disease treatment, *Eur. J. Med. Chem.* 145 (2018) 760-769.

[9] L. Ismaili, B. Refouvelet, M. Benchekroun, S. Brogi, M. Brindisi, S. Gemma, G.

Campiani, S. Filipic, D. Agbaba, G. Esteban, M. Unzeta, K. Nikolic, S. Butini, J. Marco-Contelles, Multitarget compounds bearing tacrine- and donepezil-like structural and functional motifs for the potential treatment of Alzheimer's disease, *Prog. Neurobiol.* 151 (2017) 4–34.

[10] J. Wang, Z.-M. Wang, X.-M. Li, F. Li, J.-J. Wu, L.-Y. Kong, X.-B. Wang, Synthesis and evaluation of multi-target-directed ligands for the treatment of Alzheimer's disease based on the fusion of donepezil and melatonin, *Bioorg. Med. Chem.* 24 (2016) 4324–4338.

[11] D. Alonso, I. Dorronsoro, L. Rubio, P. Muñoz, E. García-Palomero, M. Del Monte, A. Bidon-Chanal, M. Orozco, F.J. Luque, A. Castro, M. Medina, A. Martínez, Donepezil–tacrine hybrid related derivatives as new dual binding site inhibitors of AChE, *Bioorg. Med. Chem.* 13 (2005) 6588–6597.

[12] A. Cavalli, M. L. Bolognesi, S. Capsoni, V. Andrisano, M. Bartolini, E. Margotti, A. Cattaneo, M. Recanatini, C. Melchiorre, A small molecule targeting the multifactorial nature of Alzheimer's disease, *Angew. Chem., Int. Ed.* 46 (2007) 3689-3692.

[13] E. García Palomero, P. Munoz, P. Usan, P. Garcia, C. De Austria, R. Valenzuela, L. Rubio, M. Medina, A. Martínez, Beta-amyloid potent β -amyloid modulators, *Neurodegener. Dis.* 5 (2008) 153-156.

[14] C. Spuch, D. Antequera, M. I. Fernandez-Bachiller, M. I Rodríguez, E Franco Carro, A new tacrine–melatonin hybrid reduces amyloid burden and behavioral deficits in a mouse model of Alzheimer's disease, *Neurotox. Res.* 17 (2010) 421-431.

- [15] P. Camps, X. Formosa, C. Galdeano, T. Gómez, D. Munoz-Torrero, L. Ramírez, E. Viayna, E. Gómez, N. Isambert, R. Lavilla, A. Badia, M.V. Clos, M. Bartolini, F. Mancini, V. Andrisano, A. Bidon-Chanal, Ó. Huertas, T. Dafni, F. J. Luque, Tacrine-based dual binding site acetylcholinesterase inhibitors as potential disease-modifying anti-Alzheimer drug candidates, *Chemico-Biological Interactions* 187 (2010) 411–415.
- [16] Pilar Muñoz-Ruiz, L. Rubio, E. García-Palomero, Isabel Dorronsoro, M. del Monte-Millán, R. Valenzuela, P. Usán, C. de Austria, M. Bartolini, V. Andrisano, A. Bidon-Chanal, M. Orozco, F. J. Luque, M. Medina, A. Martínez, Design, synthesis, and biological evaluation of dual binding site acetylcholinesterase inhibitors: new disease-modifying agents for Alzheimer's disease, *J. Med. Chem.* 48 (2005) 7223–7233.
- [17] J.S. Lan, T. Zhang, Y. Liu, J. Yang, S.S. Xie, J. Liu, Z.Y. Miao, Y. Ding, Design, synthesis and biological activity of novel donepezil derivatives bearing N-benzyl pyridinium moiety as potent and dual binding site acetylcholinesterase inhibitors, *Eur. J. Med. Chem.* 133 (2017) 184–196.
- [18] C.B. Mishra, S. Kumari, A. Manral, A. Prakash, V. Saini, A.M. Lynn, M. Tiwari, Design, synthesis, in silico and biological evaluation of novel donepezil derivatives as multi-target-directed ligands for the treatment of Alzheimer's disease, *Eur. J. Med. Chem.* 125 (2017) 736–750.
- [19] X. Chen, S. Wehle, N. Kuzmanovic, B. Merget, U. Holzgrabe, B. König, C. A. Sotriffer, M. Decker, Acetylcholinesterase inhibitors with photoswitchable inhibition of β -amyloid aggregation, *ACS Chem. Neurosci.* 5 (2014) 377–389.
- [20] C. Galdeano, E. Viayna, I. Sola, X. Formosa, P. Camps, A. Badia, M.V. Clos, J. Relat, M. Ratia, M. Bartolini, F. Mancini, V. Andrisano, M. Salmona, C. Minguillon, G.C. Gonzalez-Munoz, M.I. Rodríguez-Franco, Huprine–tacrine heterodimers as anti-

amyloidogenic compounds of potential interest against Alzheimer's and prion Diseases, *J. Med. Chem.* 55 (2012) 661-669.

[21] G.V. De Ferrari, M. A. Canales, I. Shin, L. M. Weiner, I. Silman, N. C. Inestrosa, A structural motif of acetylcholinesterase that promotes amyloid beta-peptide fibril formation, *Biochemistry* 40 (2001) 10447-10457.

[22] M. Bartolini, C. Bertucci, C. Cavrini, V. Andrisano, beta-Amyloid aggregation induced by human acetylcholinesterase: inhibition studies, *Biochem Pharmacol.* 65 (2003) 407-416.

[23] N.C. Inestrosa, M.C. Dinamarca, A. Alvarez, Amyloid-cholinesterase interactions. Implications for Alzheimer's disease, *FEBS J.* 275 (2008) 625-632.

[24] A. Pariente, Dina J-R. Sanctussy, G. Miremont-Salame, N. Moore, F. Haramburu, A. Fourier-Reglat, Factors associated with serious adverse reactions to cholinesterase inhibitors: a study of spontaneous reporting, *CNS Drugs*, 24 (2010) 55-63.

[25] P. Bohn, N. Le Fur, G. Hagues, J. Costentin, N. Torquet, C. Papamicaël, F. Marsais, V. Levacher, Rational design of central selective acetylcholinesterase inhibitors by means of a "bio-oxidisable prodrug" strategy, *Org. Biomol. Chem.* 7 (2009) 2612-2618.

[26] P. Bohn, F. Gourand, C. Papamicaël, M. Ibazizène, M. Dhilly, V. Gembus, F. Alix, M.-L. Țîntaş, F. Marsais, L. Barré, V. Levacher, Dihydroquinoline Carbamate Derivatives as "Bio-oxidizable" Prodrugs for brain delivery of acetylcholinesterase inhibitors: [^{11}C] radiosynthesis and biological evaluation, *ACS Chem. Neurosci.* 6 (2015) 737-744.

[27] M. Node, K. Nishide, K. Fuji, E. Fujita, Hard acid and soft nucleophile system. 2. Demethylation of methyl ethers of alcohol and phenol with an aluminum halide-thiol system, *J. Org. Chem.* 45 (1980) 4275-4277.

- [28] G. L. Ellman, K. D. Courtney, Jr. V. Andres, R. M. Featherstone, A new and rapid colorimetric determination of acetylcholinesterase activity. *Biochem. Pharmacol.* 7 (1961) 88-95.
- [29] O. Trott, A. J. Olson, AutoDock Vina: improving the speed and accuracy of docking with a new scoring function, efficient optimization and multithreading, *J Comput Chem* 31 (2010) 455–61.
- [30] PyMol 0.99rc6 (DeLano Scientific, 2006, San Carlo, USA).
- [31] D. Alonso, I. Dorronsoro, L. Rubio, P. Munoz, E. García-Palomero, M. Del Monte, A. Bidon-Chanal, M. Orozco, F.J. Luque, A. Castro, M. Medina, A. Martínez, Donepezil-tacrine hybrid related derivatives as new dual binding site inhibitors of AChE, *Bioorg. Med. Chem.* 13 (2005) 6588-6597.
- [32] M. Hebda, M. Bajda, A. Wieckowska, N. Szałaj, A. Pasieka, D. Panek, J. Godyń, T. Wichur, D. Knez, S. Gobec, B. Malawska, Synthesis, molecular modelling and biological evaluation of novel heterodimeric, multiple ligands targeting cholinesterases and amyloid beta, *Molecules* 21 (2016) 410.
- [33] W. Si, T. Zhang, L. Zhang, X. Mei, M. Dong, K. Zhang, J. Ning, Design, synthesis and bioactivity of novel phthalimide derivatives as acetylcholinesterase inhibitors, *Bioorg. Med. Chem. Lett.* 26 (2016) 2380-2382.
- [34] M. Saeedi, M. Golipoor, M. Mahdavi, A. Moradi, H. Nadri, S. Emami, A. Foroumadi, A. Shafiee, Phthalimide-derived N-benzylpyridinium halides targeting cholinesterases: synthesis and bioactivity of new potential anti-Alzheimer's disease agents, *Arch. Pharm. Chem. Life Sci.* 349 (2016) 293–301.

- [35] G. Pastorin, W. Wu, S. Wieckowski, J.-P. Briand, K. Kostarelos, M. Prato, A. Bianco, Double functionalisation of carbon nanotubes for multimodal drug delivery, *Chem. Commun.* 11 (2006) 1182-1184.
- [36] A. Więckowska, K. Więckowski, M. Bajda, B. Brus, K. Sałat, P. Czerwinska, S. Gobec, B. Filipek, B. Malawska, Synthesis of new Nbenzylpiperidine derivatives as cholinesterase inhibitors with β amyloid anti-aggregation properties and beneficial effects on memory in vivo, *Bioorg. Med. Chem.* 23 (2015) 2445–2457.
- [37] Y. Tamura, L. Ching Chen, M. Fujita, Y. Kita, Synthetic application of lithiation reactions: a convenient synthesis of 3, 4-dihydro-5-hydroxycarbostyryl, 1, 2, 3, 4-tetrahydro-5-hydroxy-2-oxo-1, 7-naphthyridine, and methyl 3-methoxypyridine-4-carboxylate, *Chem. Pharm. Bull.* 30 (1982) 1257–1262.
- [38] L. Zhu, Z. Miao, C. Sheng, W. Guo, J. Yao, W. Liu, X. Che, W. Wang, P. Cheng, W. Zhang, Trifluoromethyl-promoted homocamptothecins: synthesis and biological activity, *Eur. J. Med. Chem.* 45 (2010) 2726-2732.
- [39] Marvin Sketch 17.29.0, ChemAxon Ltd (1998–2017), <http://www.chemaxon.com>.
- [40] M.F. Sanner. Python: A Programming Language for Software Integration and Development, *J. Mol. Graphics Mod.* 17 (1999) 57-61.
- [41] T.D. Pettersen, G.D. Goddard, C.C. Huang, G.S. Couch, D.M. Greenblatt, E.C. Meng, T.E. Ferrin, UCSF Chimera - a visualization system for exploratory research and analysis, *J. Comput. Chem.* 25 (2004) 1605-1612.

Highlights

- Synthesis and evaluation of anti-AChE activities for compounds **2a-p**
- Grafting point determination by SAR analysis of **2a-p** and docking studies
- Synthesis and evaluation of anti-AChE activity for compound **4** and its prodrug **3**
- Docking simulation of the dual binding site inhibitor **4** in *h*AChE